

## Bioceramics: From Concept to Clinic

Larry L. Hench<sup>★</sup>

Department of Materials Science and Engineering,  
University of Florida, Gainesville, Florida 32611

Ceramics used for the repair and reconstruction of diseased or damaged parts of the musculo-skeletal system, termed bioceramics, may be bioinert (alumina, zirconia), resorbable (tricalcium phosphate), bioactive (hydroxyapatite, bioactive glasses, and glass-ceramics), or porous for tissue ingrowth (hydroxyapatite-coated metals, alumina). Applications include replacements for hips, knees, teeth, tendons, and ligaments and repair for periodontal disease, maxillofacial reconstruction, augmentation and stabilization of the jaw bone, spinal fusion, and bone fillers after tumor surgery. Carbon coatings are thromboresistant and are used for prosthetic heart valves. The mechanisms of tissue bonding to bioactive ceramics are beginning to be understood, which can result in the molecular design of bioceramics for interfacial bonding with hard and soft tissues. Composites are being developed with high toughness and elastic modulus match with bone. Therapeutic treatment of cancer has been achieved by localized delivery of radioactive isotopes via glass beads. Development of standard test methods for prediction of long-term (20-year)

mechanical reliability under load is still needed. [Key words: bioceramics, structure, dental ceramics, interfaces, mechanics.]

### I. Introduction

MANY millennia ago, the discovery of human kind that fire would irreversibly transform clay into ceramic pottery led eventually to an agrarian society and an enormous improvement in the quality and length of life. Within the last four decades another revolution has occurred in the use of ceramics to improve the quality of life. This revolution is the innovative use of specially designed ceramics for the repair and reconstruction of diseased or damaged parts of the body. Ceramics used for this purpose are termed bioceramics. Bioceramics can be single crystals (sapphire), polycrystalline (alumina or hydroxyapatite (HA)), glass (Bioglass<sup>®\*</sup>), glass-ceramics (Ceravital<sup>®†</sup> or A/W glass-ceramic), or composites (stainless-steel-fiber-reinforced Bioglass<sup>®</sup> or polyethylene-hydroxyapatite (PE-HA)).

Ceramics and glasses have been used for a long time in the health-care industry for eye glasses, diagnostic instruments, chemical ware, thermometers, tissue culture flasks, and fiber optics for endoscopy. Insoluble porous glasses have been used as carriers for enzymes, antibodies, and antigens since they have several advantages, notably resistance to microbial attack, pH changes, solvent conditions, temperature, and packing under the high pressure which is required for rapid

R. E. Newnham—contributing editor

Manuscript No. 196865. Received March 3, 1991; approved April 23, 1991.

Supported by U.S. Air Force Office of Scientific Research under Contract No. F496290-88-C-0073.

The conducted research was reviewed and approved by the University of Florida Institutional Animal Care and Use Committee to ensure that the research procedures adhered to the standards set forth in the Guide for the Care and Use of Laboratory Animals (NIH Publication 85-23) as promulgated by the Committee on Care and Use of Laboratory Animals of the Institute of Laboratory Animal Resources, Commission on Life Sciences, National Research Council.

<sup>★</sup>Member, American Ceramic Society.

<sup>\*</sup>University of Florida, Gainesville, FL.

<sup>†</sup>Leitz GmbH, Wetzlar, FRG.



feature

**Table I. Types of Implant–Tissue Response**

If the material is toxic, the surrounding tissue dies.
If the material is nontoxic and biologically inactive (nearly inert), a fibrous tissue of variable thickness forms.
If the material is nontoxic and biologically active (bioactive), an interfacial bond forms.
If the material is nontoxic and dissolves, the surrounding tissue replaces it.

flow.<sup>1</sup> Ceramics are also widely used in dentistry as restorative materials, gold porcelain crowns, glass-filled ionomer cements, dentures, etc. In these applications they are called dental ceramics as discussed by Preston.<sup>2</sup>

This review is devoted to the use of bioceramics as implants to repair parts of the body, usually the hard tissues of the musculo–skeletal system, such as bones or teeth, although a brief review of the use of carbon coatings for replacement of heart valves is also included. Dozens of ceramic compositions have been tested,<sup>1,3</sup> however, few have achieved human clinical application. It is now known that clinical success requires the simultaneous achievement of a stable interface with connective tissue and a match of the mechanical behavior of the implant with the tissue to be replaced.

## II. Types of Bioceramics–Tissue Attachment

The mechanism of tissue attachment is directly related to the type of tissue response at the implant interface.<sup>1</sup> No material implanted in living tissues is inert; all materials elicit a response from living tissues. The four types of response (Table I) allow different means of achieving attachment of prostheses to the musculo–skeletal system. Table II summarizes the attachment mechanisms, with examples.

A comparison of the relative chemical activity of these different types of bioceramics is given in Fig. 1. The relative reactivity shown in Fig. 1(a) correlates very closely with the rate of

formation of an interfacial bond of implants with bone (Fig. 1(b)).<sup>4</sup> Figure 1(b) will be discussed in more detail in Section VIII.

The relative level of reactivity of an implant influences the *thickness* of the interfacial zone or layer between the material and tissue. Analysis of failure of implant materials during the last 20 years generally shows failure originating from the biomaterial–tissue interface.<sup>4,5</sup> When a biomaterial is nearly inert (type 1 in Table II and Fig. 1) and the interface is not chemically or biologically bonded, there is relative movement and progressive development of a nonadherent fibrous capsule in both soft and hard tissues. Movement at the biomaterial–tissue interface eventually leads to deterioration in function of the implant or the tissue at the interface or both. The thickness of the nonadherent capsule varies greatly depending upon both material (Fig. 2) and extent of relative motion.

The fibrous tissue at the interface with dense, medical-grade alumina implants can be very thin.<sup>3,6</sup> Consequently, as discussed later, if alumina implants are implanted with a very tight mechanical fit and are loaded primarily in compression, they are successful clinically. In contrast, if a type 1, nearly inert, implant is loaded such that interfacial movement can occur, the fibrous capsule can become several hundred micrometers thick and the implant loosens quickly. Loosening invariably leads to clinical failure, for a variety of reasons, including fracture of the implant or the bone adjacent to the implant. Bone at an interface with a type 1, nearly inert, implant is very often structurally weak because of disease, localized death of bone (especially if so-called bone cement, poly(methyl methacrylate) (PMMA) is used), or stress shielding when the higher elastic modulus of the implant prevents the bone from being loaded properly.

The concept behind nearly inert, microporous bioceramics (type 2 in Table II and Fig. 1) is the ingrowth of tissue into pores on the surface or throughout the implant, as originated by Hulbert *et al.*<sup>3</sup> many years ago. The increased interfacial area between the implant and the tissues results in an increased inertial resistance to movement of the device in the tissue. The interface is established by the living tissue in the pores. Figure 3 shows living bone grown into the pores of an alumina bioceramic. This method of attachment is often termed biological fixation. It is capable of withstanding more complex stress states than type 1 implants, which achieve only morphological fixation." The limitation associated with type 2 porous implants, however, is that, for the tissue to remain

**Table II. Types of Bioceramics –Tissue Attachment and Bioceramic Classification**

Type of bioceramic	Type of attachment	Example
1	Dense, nonporous, nearly inert ceramics attach by bone growth into surface irregularities by cementing the device into the tissues, or by press fitting into a defect (termed morphological fixation).	Al <sub>2</sub> O <sub>3</sub> (single crystal and polycrystalline)
2	For porous inert implants bone ingrowth occurs, which mechanically attaches the bone to the material (termed biological fixation).	Al <sub>2</sub> O <sub>3</sub> (porous polycrystalline) Hydroxyapatite-coated porous metals
3	Dense, nonporous, surface-reactive ceramics, glasses, and glass-ceramics attach directly by chemical bonding with the bone (termed bioactive fixation).	Bioactive glasses Bioactive glass-ceramics Hydroxyapatite
4	Dense, nonporous (or porous), resorbable ceramics are designed to be slowly replaced by bone.	Calcium sulfate (plaster of Paris) Tricalcium phosphate Calcium phosphate salts

viable and healthy, it is necessary for the pores to be greater than 100 to 150  $\mu\text{m}$  in diameter (Fig. 2). The large interfacial area required for the porosity is due to the need to provide a blood supply to the ingrown connective tissue. Vascular tissue does not appear in pores which measure less than 100  $\mu\text{m}$ . If micromovement occurs at the interface of a porous implant, tissue is damaged, the blood supply may be cut off, tissues die, inflammation ensues, and the interfacial stability can be destroyed. When the material is a metal, the large increase in surface area can provide a focus for corrosion of the implant and loss of metal ions into the tissues, which may cause a variety of medical problems.<sup>7,9</sup> These potential problems can be diminished by using a bioactive ceramic material such as HA as a coating on the porous metal, as first shown by Ducheyne *et al.*<sup>9</sup> The HA coating also speeds the rate of bone formation in the pores. However, the fraction of large porosity required for bone growth in any material degrades the strength of the material. Consequently, this approach to solving interfacial stability is best when used as porous coatings or when used as unloaded space fillers in tissues.

Resorbable biomaterials (type 4 in Table II and Fig. 1) are designed to degrade gradually over a period of time and be replaced by the natural host tissue.<sup>10-13</sup> This leads to a very thin or nonexistent interfacial thickness (Fig. 2). This is the optimal solution to the problem of biomaterials if the requirements of strength and short-term performance can be met. Natural tissues can repair themselves and are gradually replaced throughout life by a continual turnover of cell populations. As we grow older, the replacement of cells and tissues is slower and less efficient, which is why parts "wear out," unfortunately some faster than others. Thus, resorbable biomaterials are based on the same principles of repair

which have evolved over millions of years. Complications in the development of resorbable bioceramics are (1) maintenance of strength and the stability of the interface during the degradation period and replacement by the natural host tissue and (2) matching resorption rates to the repair rates of body tissues (Fig. 1(a)), which themselves vary enormously. Some dissolve too rapidly and some too slowly. Because large quantities of material may be replaced, it is also essential that a resorbable biomaterial consists only of metabolically acceptable substances. This criterion imposes considerable limitations on the compositional design of resorbable biomaterials. Successful examples are resorbable polymers such as

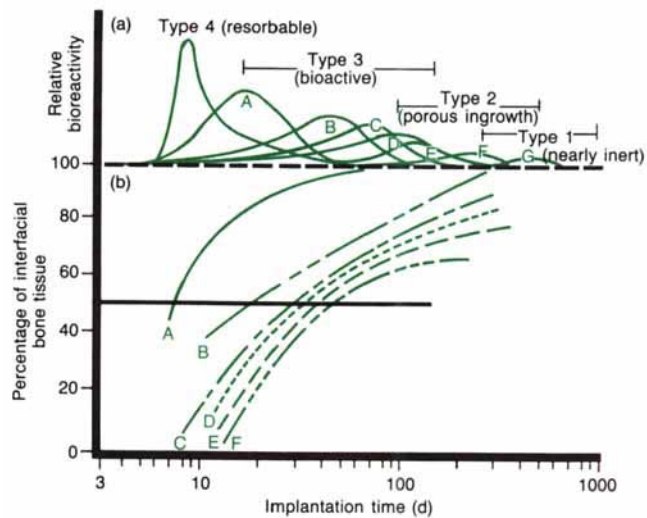


**Fig. 1.** Bioactivity spectrum for various bioceramic implants: (a) relative rate of bioreactivity and (b) time dependence of formation of bone bonding at an implant interface ((A) 45S5 Bioglass®, (B) KGS Ceravital®, (C) 55S4.3 Bioglass®, (D) A/W glass-ceramic, (E) HA, (F) KGX Ceravital®, and (G)  $\text{Al}_2\text{O}_3\text{-Si}_3\text{N}_4$ ).

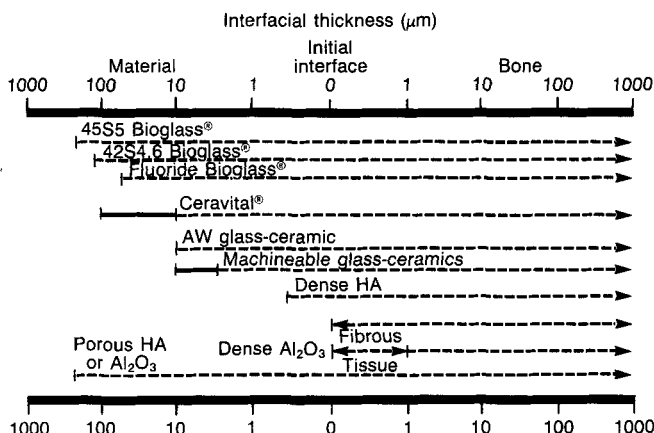


**Fig. 2.** Comparison of interfacial thickness of reaction layer of bioactive implants or fibrous tissue of inactive bioceramics in bone.

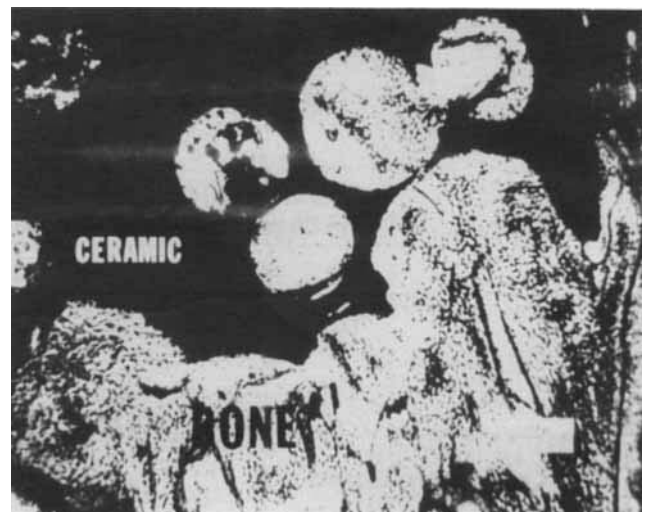


**Fig. 3.** Ingrowth of bone within  $>100\text{-}\mu\text{m}$  pores of alumina bioceramic. (Photograph courtesy of S. Hulbert.)



poly(lactic acid)–poly(glycolic acid) (PLA-PGA) used for sutures, which are metabolized to carbon dioxide and water and therefore are able to function for a period and then dissolve and disappear. Porous or particulate calcium phosphate ceramic materials such as tricalcium phosphate (TCP) are successful materials for resorbable hard-tissue replacements when only low mechanical strength is required, such as in some repairs of the jaw or head.<sup>10–13</sup>

Another approach to the solution of the problems of interfacial attachment is the use of bioactive materials (type 3 in Table II and Fig. 1). The concept of bioactive materials is intermediate between resorbable and bioinert.<sup>1,4,5</sup> A bioactive material is one that elicits a specific biological response at the interface of the material which results in the formation of a bond between the tissues and the material (shown first in 1969).<sup>14</sup> This concept has now been expanded to include a large number of bioactive materials with a wide range of rates of bonding and thickness of interfacial bonding layers (Figs. 1 and 2). They include<sup>4,5</sup> bioactive glasses such as Bioglass®; bioactive glass-ceramics such as Ceravital®, A/W glass-ceramic, or machineable glass-ceramics; dense HA such as durapatite or Calcitite®<sup>†</sup>, or bioactive composites such as Palavital®<sup>‡</sup>, stainless-steel-fiber-reinforced Bioglass®; and PE–HA mixtures. All of these bioactive materials form an interfacial bond with adjacent tissue. However, the time dependence of bonding, the strength of the bond, the mechanism of bonding, and the thickness of the bonding zone differ for the various materials.

It is important to recognize that relatively small changes in the composition of a biomaterial can affect dramatically whether it is bioinert, resorbable, or bioactive. These compositional effects on surface reactions are discussed in Section V.

<sup>†</sup>Calatek, Inc., San Diego, CA.

<sup>‡</sup>Leitz GmbH.

### III. Nearly Inert Crystalline Bioceramics

High-density, high-purity (>99.5%) alumina ( $\alpha$ -Al<sub>2</sub>O<sub>3</sub>) was the first bioceramic widely used clinically. It is used in load-bearing hip prostheses and dental implants because of its combination of excellent corrosion resistance, good biocompatibility, high wear resistance, and high strength.<sup>1,3,6,15–18</sup> Although some dental implants are single-crystal sapphire,<sup>19</sup> most alumina devices are very-fine-grained polycrystalline  $\alpha$ -Al<sub>2</sub>O<sub>3</sub>. A very small amount of magnesia (<0.5%) is used as an aid to sintering and to limit grain growth during sintering.

Strength, fatigue resistance, and fracture toughness of polycrystalline  $\alpha$ -Al<sub>2</sub>O<sub>3</sub> are a function of grain size and percentage of sintering aid, i.e., purity. Alumina with an average grain size of <4  $\mu$ m and >99.7% purity exhibits good flexural strength and excellent compressive strength. These and other physical properties are summarized in Table III<sup>6</sup> with the International Standards Organization (ISO) requirements for alumina implants. Extensive testing has shown that alumina implants which meet or exceed ISO standards have excellent resistance to dynamic and impact fatigue and also resist subcritical crack growth.<sup>20</sup> An increase in the average grain size to >7  $\mu$ m can decrease mechanical properties by about 20%. High concentration of sintering aids must be avoided because they remain in the grain boundaries and degrade fatigue resistance, especially in a corrosive physiological environment.<sup>1</sup>

Methods exist for lifetime predictions and statistical design of proof tests for load-bearing ceramics. Applications of these techniques show that specific prosthesis load limits can be set for an alumina device based upon the flexural strength of the material and its use environment.<sup>21</sup> Load-bearing lifetimes of 30 years at 12000-N loads, similar to those expected in hip joints, have been predicted.<sup>6</sup> Results from aging and fatigue studies show that it is essential that alumina implants be produced at the highest possible standards of qual-

**Table III. Physical Characteristics of Alumina and Partially Stabilized Zirconia (PSZ) Bioceramics**

	High-alumina ceramics*	ISO alumina standard 6474	PSZ*	Cortical bone <sup>1</sup>	Cancellous bone <sup>2</sup>
Content (percent by weight)	Al <sub>2</sub> O <sub>3</sub> > 99.8	Al <sub>2</sub> O <sub>3</sub> $\geq$ 99.50	ZrO <sub>2</sub> > 97		
Density (g/cm <sup>3</sup> )	> 3.93	$\geq$ 3.90	5.6–6.12	1.6–2.1	
Average grain size ( $\mu$ m)	3–6	< 7	1		
Surface roughness, R <sub>a</sub> ( $\mu$ m)	0.02		0.008		
Hardness (Vickers), HV	2300	> 2000	1300		
Compressive strength (MPa)	4500				2–12
Bending strength (MPa)	550	400	1200	50–150	
(after testing in Ringer's solution)					
Young's Modulus (GPa)	380		200	7–25	0.05–0.5
Fracture toughness, K <sub>IC</sub> (MPa · m <sup>-1/2</sup> )	5–6		15	2–12	
Slow crack growth, n (unitless)	30–52		65		

\*Reference 6. <sup>1</sup>References 120 and 121. <sup>2</sup>Reference 122.

ity assurance, especially if they are to be used as orthopedic prostheses in younger patients (<50 years old).

Alumina has been used in orthopedic surgery for nearly 20 years, motivated largely by (1) its excellent type 1 biocompatibility and very thin capsule formation (Fig. 2) which permits cementless fixation of prostheses<sup>3</sup> and (2) its exceptionally low coefficients of friction and wear rates.<sup>3,6</sup>

The superb tribologic properties (friction and wear) of alumina occur only when the grains are very small (<4  $\mu\text{m}$ ) and have a very narrow size distribution. These conditions lead to very low surface roughness values ( $R_a \leq 0.02 \mu\text{m}$ , Table III). If large grains are present, they can pull out and lead to very rapid wear because of local dry friction and abrasion caused by the alumina grains in the joint-bearing surfaces.<sup>6</sup>

Alumina on alumina load-bearing wearing surfaces, such as in hip prostheses, must have a very high degree of sphericity produced by grinding and polishing the two mating surfaces together. The alumina ball and socket in a hip prosthesis are polished together and used as a pair. The long-term coefficient of friction of an alumina-alumina joint decreases with time and approaches the values of a normal joint. This leads to wear of alumina on alumina articulating surfaces that are nearly 10 times lower than metal-PE surfaces (Fig. 4).

Low wear rates have led to widespread use in Europe of alumina non-cemented cups press fitted into the acetabulum (socket) of the hip. The cups are stabilized by bone growth into grooves or around pegs. The mating femoral ball surface is also of alumina which is bonded to a metallic stem. Long-term results in general are excellent, especially for younger patients. However, Christel *et al.*<sup>6</sup> caution that stress shielding of the bone can occur. This is due to the high Young's modulus of alumina (Table III), which prevents the bone from being loaded, a requirement for bone to remain healthy and strong. The Young's modulus of cortical bone ranges between 7 and 25 GPa (as discussed in Section X) which is 10 to 50 times lower than alu-

mina. Christel *et al.*<sup>6</sup> report that stress shielding may be responsible for cancellous bone atrophy and loosening of the acetabular cup in older patients with senile osteoporosis or rheumatoid arthritis. Consequently, it is essential that the age of the patient, nature of the disease of the joint, and biomechanics of the repair be considered carefully before any prosthesis is used, including those made from alumina ceramics. In the United States, the primary use of alumina is for the ball of the hip joint (Fig. 5), with the acetabular component being ultrahigh-molecular-weight PE.

Other clinical applications of alumina prostheses, reviewed by Hulbert *et al.*,<sup>3</sup> include knee prostheses, bone screws, alveolar ridge (jaw bone) and maxillo-facial reconstruction, ossicular (middle ear) bone substitutes, keratoprostheses (corneal replacements), segmental bone replacements, and blade and screw and post-type dental implants.

#### IV. Porous Ceramics

The potential advantage offered by a porous ceramic implant (type 2, Table II, Figs. 1 and 2) is its inertness combined with the mechanical stability of the highly convoluted interface developed when bone grows into the pores of the ceramic. Mechanical requirements of prostheses, however, severely restrict the use of low-strength porous ceramics to low-load- or non-load-bearing applications. Studies show that, when load bearing is not a primary requirement, nearly inert porous ceramics can provide a functional implant.<sup>1,3,22-24</sup> When pore sizes exceed 100  $\mu\text{m}$ , bone will grow within the inter-connecting pore channels near the surface and maintain its vascularity and long-term viability (Fig. 3). In this manner the implant serves as a structural bridge and model or scaffold for bone formation. The microstructures of certain corals make an almost ideal investment material for the casting of

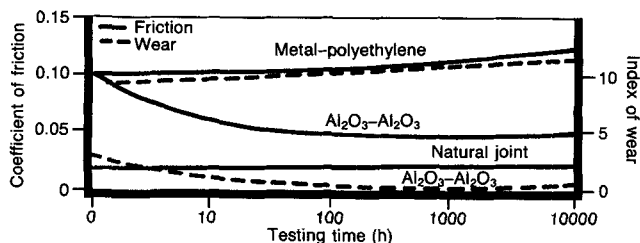


Fig. 4. Time dependence of (—) coefficient of friction and (---) index of wear of alumina-alumina versus metal-PE hip joint (in vitro testing).



Fig. 5. Medical-grade alumina used as femoral balls in total hip replacement. Note three alternative types of metallic stems used for morphological fixation. (Photograph courtesy of J. Parr.)

structures with highly controlled pore sizes. White *et al.*<sup>23</sup> developed the replamineform process to duplicate the porous microstructure of corals that have a high degree of uniform pore size and interconnection. The first step is to machine the coral with proper microstructure into the desired shape. The most promising coral genus, *Porites*, has pores with a size range of 140 to 160  $\mu\text{m}$ , with all the pores interconnected.<sup>22</sup> Another interesting coral genus, *Goniopora*, has a larger pore size, ranging from 200 to 1000  $\mu\text{m}$ . The machined coral shape is fired to drive off carbon dioxide from the limestone ( $\text{CaCO}_3$ ), forming calcia, while maintaining the microstructure of the original coral. The calcia structure serves as an investment material for forming the porous material. After the desired material is cast into the pores, the calcia is easily removed from the material by dissolving it in dilute hydrochloric acid. The primary advantages of the replamineform process are that the pore size and microstructure are uniform and controlled, and there is complete interconnection of the pores. Replamineform porous materials of  $\alpha\text{-Al}_2\text{O}_3$ , titania, calcium phosphates, polyurethane, silicone rubber, PMMA, and Co–Cr alloys have been used as bone implants with the calcium phosphates being the most acceptable.<sup>22–25</sup>

Porous ceramic surfaces can also be prepared by mixing soluble metal or salt particles into the surface. The pore size and structure are determined by the size and shape of the soluble particles that are subsequently removed with a suitable etchant. The porous surface layer produced by this technique is an integral part of the underlying dense ceramic phase.

Materials such as alumina may also be made porous by using a suitable foaming agent that evolves gases during heating. Porous alumina and calcium aluminates used by Hulbert and colleagues<sup>26–29</sup> in some of their bone ingrowth studies were produced by mixing powdered calcium carbonate with fine alumina powder. A firing time of 20 h at approximately 1450° to 1500°C produced a foamed material with pore size and volume fraction (33% to 48% of porosity) determined by the size and concentration of the original calcium carbonate particles.

Porous materials are weaker than the equivalent bulk form. As the porosity increases the strength of the material decreases rapidly as indicated by the Ryskewitch equation:

$$\sigma = \sigma_0 e^{-cp} \quad (1)$$

where  $\sigma$  is strength,  $\sigma_0$  is strength at zero porosity,  $c$  is constant, and  $p$  is porosity.

Much surface area is also exposed, so that the effects of the environment

on decreasing the strength become much more important than for dense, nonporous materials.<sup>1</sup> The in vitro aging of porous alumina in saline solution for periods of 4 weeks as well as in vivo testing for up to 3 months reduces strength of porous alumina samples by 35% to 40%. Permeation into the micropores of seemingly dense alumina can also result in marked reductions in tensile strength. Another porous, high-strength ceramic, calcia-stabilized zirconia, also undergoes significant decreases in strength with time as do calcium aluminates.<sup>1</sup> Aging of porous ceramics, with their subsequent decrease in strength, poses questions as to the successful long-term application of porous materials unless they are designed to be resorbable, e.g., are made of calcium salts such as TCP.

## V. Bioactive Glasses and Glass-Ceramics

Certain compositions of glasses, ceramics, glass-ceramics, and composites have been shown to bond to bone.<sup>1,3,4,5,7,9–14,25,30–40</sup> These materials have become known as bioactive ceramics.<sup>4,5,25,41</sup> Some even more specialized compositions of bioactive glasses will bond to soft tissues as well as bone.<sup>35,42</sup> A common characteristic of bioactive glasses and bioactive ceramics is a time-dependent, kinetic modification of the surface that occurs upon implantation.<sup>4,5</sup> The surface forms a biologically active hydroxycarbonate apatite (HCA) layer which provides the bonding interface with tissues. The HCA phase that forms on bioactive implants is equivalent chemically and structurally to the mineral phase in bone. It is that equivalence which is responsible for interfacial bonding.

Materials that are bioactive develop an adherent interface with tissues that resists substantial mechanical forces. In many cases the interfacial strength of adhesion is equivalent to or greater than the cohesive strength of the implant material or the tissue bonded to the bioactive implant. Figures 6 and 7 show bioactive implants bonded to bone with adherence at the interface sufficient to resist mechanical fracture. Failure occurs either in the implant (Fig. 6) or in the bone (Fig. 7) but almost never at the interface.

Bonding to bone was first demonstrated for a certain compositional range of bioactive glasses which contained  $\text{SiO}_2$ ,  $\text{Na}_2\text{O}$ ,  $\text{CaO}$ , and  $\text{P}_2\text{O}_5$  in specific proportions (Table IV).<sup>16</sup> There were three key compositional features to these glasses that distinguished them from traditional  $\text{Na}_2\text{O}$ – $\text{CaO}$ – $\text{SiO}_2$  glasses: (1) less than 60 mol%  $\text{SiO}_2$ , (2) high- $\text{Na}_2\text{O}$  and high- $\text{CaO}$  content, and (3) high- $\text{CaO}/\text{P}_2\text{O}_5$  ratio. These compositional features made the sur-



face highly reactive when exposed to an aqueous medium.

Many bioactive silica glasses are based upon the formula called 45S5 (signifying 45 wt% SiO<sub>2</sub>, S as the network former, and a 5 to 1 molar ratio of Ca to P). Glasses with substantially lower molar ratios of Ca to P (in the form of CaO and P<sub>2</sub>O<sub>5</sub>) do not bond to bone.<sup>43</sup> However, substitutions in the 45S5 formula of 5 to 15 wt% B<sub>2</sub>O<sub>3</sub> for SiO<sub>2</sub> or 12.5 wt% CaF<sub>2</sub> for CaO or crystallizing the various bioactive glass compositions to form glass-ceramics has no measurable effect on the ability of the material to form a bone bond.<sup>43</sup> However, addition of as little as 3 wt% Al<sub>2</sub>O<sub>3</sub> to the 45S5 formula prevents bonding.<sup>5,31,43-46</sup>

The compositional dependence (in weight percent) of bone bonding and soft-tissue bonding for the Na<sub>2</sub>O-CaO-P<sub>2</sub>O<sub>5</sub>-SiO<sub>2</sub> glasses is illustrated in Fig. 8. All glasses in Fig. 8 contain a constant 6 wt% of P<sub>2</sub>O<sub>5</sub>. Compositions in the middle of the diagram (region A) form a bond with bone. Consequently, region A is termed the bioactive-bone-bonding boundary. Silica glasses within

region B (such as window, bottle, or microscope slide glasses) behave as type 1, nearly inert materials and elicit a fibrous capsule at the implant-tissue interface. Glasses within region C are resorbable and disappear within 10 to 30 d of implantation. Glasses within region D are not technically practical and therefore have not been tested as implants.

The collagenous constituent of soft tissues can strongly adhere to the bioactive silica glasses which lie within the compositional range (dashed line) shown in Fig. 8. Figure 9 shows collagen from a 10-d in vitro test-tube experiment bonded to a 45S5 Bioglass® surface by agglomerates of HCA crystallites growing on the surface. The collagen fibrils are woven into the interface by growth of the HCA layer (Fig. 9(a)). The dense HCA-collagen agglomerates (Fig. 9(b)) mimic the nature of bonding between tendons and ligaments, composed entirely of collagen fibrils, and bone which is a composite of HCA crystals and collagen.<sup>47,48</sup> The composite interface composed of HCA collagen on the

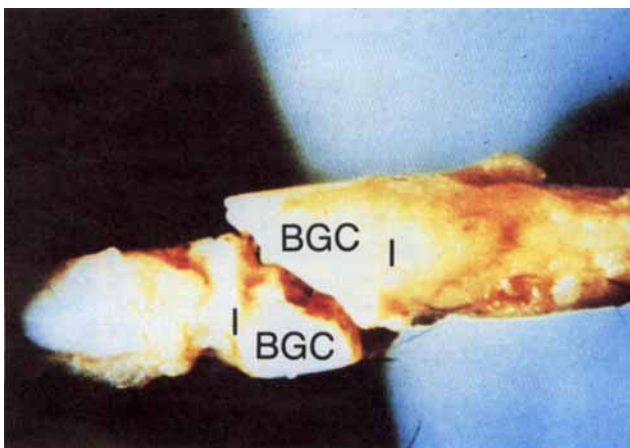


**Fig. 6.** Fracture of (BGC) 45S5 Bioglass®-ceramic segmental bone replacement in monkey due to impact torsional loading.<sup>76</sup> Note (I) bonded interface. (Photograph courtesy G. Piotrowski.)

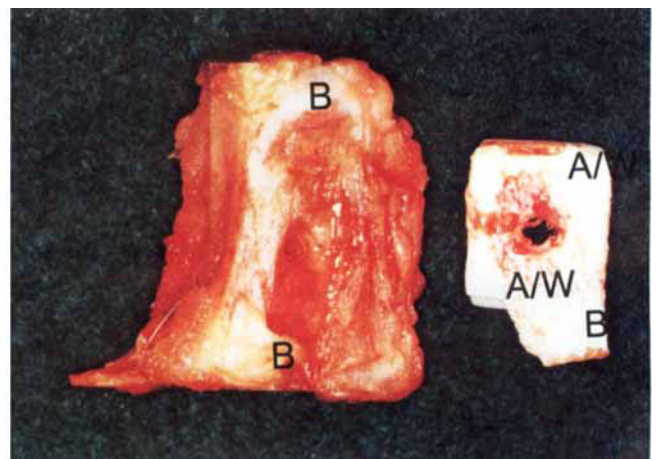


**Fig. 7.** Interfacial adherence of A/W bioactive glass-ceramic is stronger than either (B) bone or (A/W) implant. (Photograph courtesy T. Yamamura.)

**Table IV. Composition of Bioactive Glasses and Glass-Ceramics (wt%)**

Component	45S5 Bioglass®	45S5.4F Bioglass®	45B15S5 Bioglass®	52S4.6 Bioglass®	55S4.3 Bioglass®	KGC Ceravital®	KGS Ceravital®	KGy213 Ceravital®	A/W glass-ceramic	MB glass-ceramic	S45P7
SiO <sub>2</sub>	45	45	30	52	55	46.2	46	38	34.2	19-52	45
P <sub>2</sub> O <sub>5</sub>	6	6	6	6	6	20.2	33	31	16.3	4-24	7
CaO	24.5	14.7	24.5	21	19.5	25.5	16	13.5	44.9	9-3	22
Ca(PO <sub>3</sub> ) <sub>2</sub>											
CaF <sub>2</sub>		9.8							0.5		
MgO						2.9			4.6	5-15	
MgF <sub>2</sub>											
Na <sub>2</sub> O	24.5	24.5	24.5	21	19.5	4.8	5	4		3-5	24
K <sub>2</sub> O						0.4				3-5	
Al <sub>2</sub> O <sub>3</sub>								7		12-33	
B <sub>2</sub> O <sub>3</sub>			15								2
Ta <sub>2</sub> O <sub>5</sub> /TiO <sub>2</sub>								6.5			
Structure	Glass and glass-ceramic	Glass	Glass	Glass		Glass-ceramic	Glass-ceramic	Glass-ceramic	Glass-ceramic	Glass-ceramic	
Reference	14	14, 56	57, 58	44	44	5	5	5	36	32	54

bioactive glass is approximately 30 to 60  $\mu\text{m}$  of the 100- to 200- $\mu\text{m}$  total interfacial thickness (Fig. 2). This junction thickness is equivalent to that at naturally occurring interfaces where a transition occurs between materials (tendons and ligaments) with a low Young's modulus and bone with a moderately high Young's modulus. The thickness of the hard-tissue–bioactive ceramic interfaces is indicated in Fig. 2 for several compositions. The interfacial thickness decreases as the bone-bonding boundary shown in Fig. 8 is approached.

Gross and co-workers<sup>5,31,49–52</sup> have shown that a range of low-alkali (0 to 5 wt%), bioactive silica glass-ceramics (Ceravital<sup>®</sup>) also bond to bone. They find that small additions of  $\text{Al}_2\text{O}_3$ ,  $\text{Ta}_2\text{O}_5$ ,  $\text{TiO}_2$ ,  $\text{Sb}_2\text{O}_3$ , or  $\text{ZrO}_2$  inhibit bone bonding (Table IV, Fig. 1). A two-phase silica–phosphate glass-ceramic com-

posed of apatite ( $\text{Ca}_{10}(\text{PO}_4)_6(\text{OH},\text{F}_2)$ ) and wollastonite ( $\text{CaO}\cdot\text{SiO}_2$ ) crystals and a residual  $\text{SiO}_2$  glassy matrix, termed A/W glass-ceramic by the Kyoto University team in Japan,<sup>34,36–40</sup> also bonds with bone and has very high interfacial bond strength.<sup>37,38</sup> Addition of  $\text{Al}_2\text{O}_3$  or  $\text{TiO}_2$  to the A/W glass-ceramic also inhibits bone bonding, whereas incorporation of a second phosphate phase,  $\beta$ -whitlockite ( $3\text{CaO}\cdot\text{P}_2\text{O}_5$ ), does not.

Another multiphase bioactive silica–phosphate glass-ceramic containing phlogopite ( $(\text{Na},\text{K})\text{Mg}_3(\text{AlSi}_3\text{O}_{10})\text{F}_2$ ), a mica, and apatite crystals, bonds to bone even though  $\text{Al}_2\text{O}_3$  is present in the composition.<sup>32</sup> However, the  $\text{Al}^{3+}$  ions are incorporated within the crystal phase and do not alter the surface reaction kinetics of the material. An advantage of these mica-containing glass-ceramics, developed by the Friedrich Schiller University, Jena, Federal Republic of Germany, is their easy machinability.<sup>53</sup> Additional compositions of bioactive glasses have been developed at Abo Akademi, Turku, Finland, for coating onto dental alloys.<sup>45,54,55</sup> Compositions of these various bioactive glasses and glass-ceramics are compared in Table IV.

## VI. Interfacial Reaction Kinetics

The literature base for stage 1 (ion exchange) and stage 2 (silica network dissolution) reactions (see Table V) is quite extensive, as reviewed in Refs. 60 to 64. Measurements of stage 3, silica repolymerization, are less extensive<sup>65,66</sup> but fairly conclusive. Surface compositional profiles resulting from stage 1 through stage 4 reactions have been measured for numerous glass compositions.<sup>60–70</sup> The effects of addition of sparingly soluble cations, such as Mg, Ca, and Al, to glasses and/or

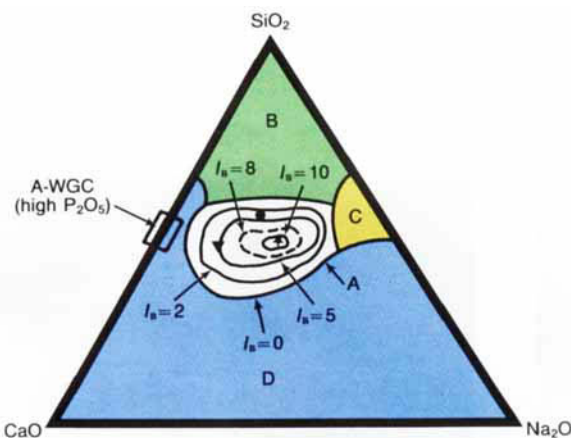
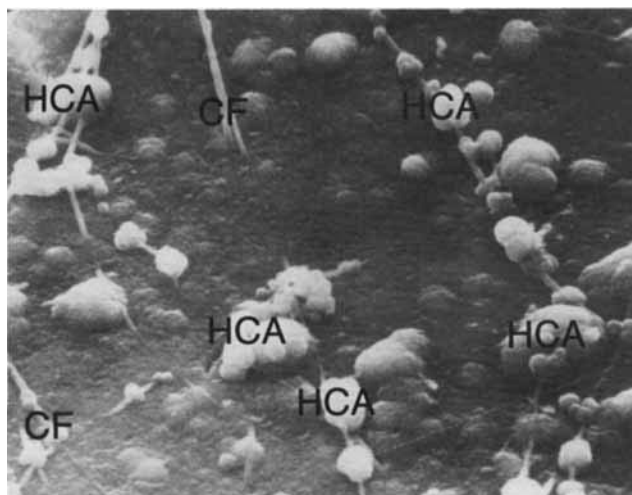
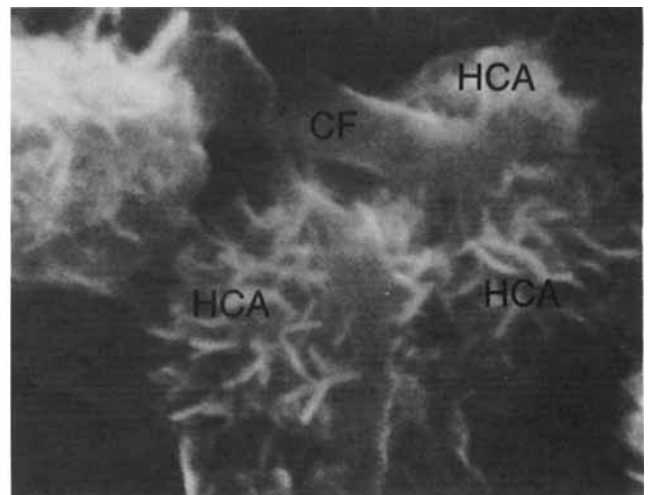


**Fig. 8.** Compositional dependence (in weight percent) of bone bonding and soft-tissue bonding of bioactive glasses and glass-ceramics. All compositions in region A have a constant 6 wt% of  $\text{P}_2\text{O}_5$ . A/W glass-ceramic has higher  $\text{P}_2\text{O}_5$  content (see Table IV for details). Region E (soft-tissue bonding) is inside the dashed line where  $I_B > 8$  ( $\star$ ) 45S5 Bioglass<sup>®</sup>, ( $\nabla$ ) Ceravital<sup>®</sup>, ( $\circ$ ) 55S4.3 Bioglass<sup>®</sup>, and (---) soft-tissue bonding;  $I_B = 100/t_{0.5\text{cb}}$ .



(A)



(B)

**Fig. 9.** (a) SEM micrograph of collagen fibrils incorporated within the HCA layer growing on a 45S5 Bioglass<sup>®</sup> substrate in vitro. (b) Close-up ( $\sim 11300\times$ ) of the HCA crystals bonding to a collagen fibril. (Photographs courtesy of C. Pantano.)



reaction solutions are also well documented.<sup>60,61,63,64</sup> The effects of glass-crystal interfaces on overall reaction rates have been measured for simple systems,<sup>59</sup> but not on complex, multiphase bioactive glass-ceramics or bioactive composites.

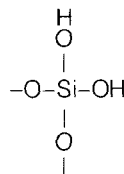
Table V summarizes the time-dependent changes of *only* a single-phase amorphous or glassy material. If one desires to understand a multiphase bioactive implant, such as Ceravital®, A/W glass-ceramic, polycrystalline sintered HA, or a bioactive composite, it is necessary to establish the time-dependent surface changes for each phase *and* each interface between the phases. The biological environment may degrade a phase or an interface preferentially leading to grain-boundary degradation for certain bioactive glass-ceramics, as discussed by Gross *et al.*<sup>5</sup>

### VII. Example of Glass-Surface Reaction Kinetics (45S5 Bioglass®)

The original bioactive glass 45S5 has been used as a baseline for most surface studies, largely because it is single phase and has only four components (Na<sub>2</sub>O, CaO, P<sub>2</sub>O<sub>5</sub>, SiO<sub>2</sub>). This simple composition (Table IV) also has the highest *in vivo* bioactivity index (*I<sub>B</sub>*) as discussed later. Recent investigations<sup>66,70,71</sup> show quite clearly the reaction sequence depicted by Eq. (1) for 45S5 Bioglass® exposed to tris(hydroxymethyl)aminomethane buffer solution (TBS) that does not contain Ca or P ions (TBS). Figures 10 and 11 summarize these findings, determined using Fourier transform infrared (FTIR) spectroscopy of the reacted surface as a function of exposure time. All five reaction stages are clearly delineated by changes in the vibrational modes of

the chemical species in the surface. Figure 10 shows the 45S5 glass surface before reaction (0 h), after 1 h, and after 2 h. The peak identifications are based upon previous assignments of IR spectra.<sup>73-75</sup> The alkali-ion-hydrogen-ion exchange and network dissolution (stages 1 and 2 in Table V) very rapidly reduces the intensity of the Si-O-Na and Si-O-Ca vibrational modes and replaces them with Si-OH bonds with one nonbridging oxygen (NBO) ion. Alkali content is depleted to a depth >0.5 μm within a few minutes.

As the stage 1 and 2 reactions continue, the Si-OH single, NBO modes are replaced with



i.e., Si-2NBO stretching vibrations which are in the range of 930 cm<sup>-1</sup>, decreasing to 880 cm<sup>-1</sup>. By 20 min, the Si-2NBO vibrations (Fig. 11) are largely replaced by a new mode assigned to the Si-O-Si bond vibration between two adjacent SiO<sub>4</sub> tetrahedra. Thus, this new vibrational mode corresponds to the formation of the silica-gel layer by the stage 3 (Table V) polycondensation reaction between neighboring surface silanol groups. This mode decreases in frequency until it is hidden by the growing apatite layer after 1 h.

As early as 10 min, a P-O bending vibration associated with formation of an amorphous calcium phosphate layer appears. This is due to precipitation from solution (stage 4 in Table V).

**Table V. Reaction Stages of a Bioactive Implant**

Stage	Reaction
1	Rapid exchange of Na <sup>+</sup> or K <sup>+</sup> with H <sup>+</sup> or H <sub>3</sub> O <sup>+</sup> from solution: $\text{Si-O-Na}^+ + \text{H}^+ + \text{OH}^- \rightarrow \text{Si-OH} + \text{Na}^+(\text{solution}) + \text{OH}^-$ This stage is usually controlled by diffusion and exhibits a $t^{-1/2}$ dependence. <sup>60-63</sup>
2	Loss of soluble silica in the form of Si(OH) <sub>4</sub> to the solution, resulting from breaking of Si-O-Si bonds and formation of Si-OH (silanols) at the glass solution interface: $\text{Si-O-Si} + \text{H}_2\text{O} \rightarrow \text{Si-OH} + \text{OH-Si}$ This stage is usually controlled by interfacial reaction and exhibits a $t^{1/2}$ dependence. <sup>60,61</sup>
3	Condensation and repolymerization of a SiO <sub>2</sub> -rich layer on the surface depleted in alkalis and alkaline-earth cations: $\begin{array}{ccccccc} \text{O} & & \text{O} & & \text{O} & & \text{O} \\   & &   & &   & &   \\ \text{O-Si-OH} & + & \text{HO-Si-O} & \rightarrow & \text{O-Si-O-Si-O} & + & \text{H}_2\text{O} \\   & &   & &   & &   \\ \text{O} & & \text{O} & & \text{O} & & \text{O} \end{array}$
4	Migration of Ca <sup>2+</sup> and PO <sub>4</sub> <sup>3-</sup> groups to the surface through the SiO <sub>2</sub> -rich layer forming a CaO-P <sub>2</sub> O <sub>5</sub> -rich film on top of the SiO <sub>2</sub> -rich layer, followed by growth of the amorphous CaO-P <sub>2</sub> O <sub>5</sub> -rich film by incorporation of soluble calcium and phosphates from solution. <sup>67,68,71</sup>
5	Crystallization of the amorphous CaO-P <sub>2</sub> O <sub>5</sub> film by incorporation of OH <sup>-</sup> , CO <sub>3</sub> <sup>2-</sup> , or F <sup>-</sup> anions from solution to form a mixed hydroxyl, carbonate, fluorapatite layer.

Clark *et al.*<sup>67</sup> showed, using Auger electron spectroscopy (AES) and Ar-ion-beam milling, that, even by 2 min, calcium and phosphate enrichment occurred on the sample surface to a depth of approximately 20 nm. Ogino *et al.*<sup>67</sup> showed that, by 1 h, the calcium phosphate layer grew to 200 nm in thickness. The bilayer films of calcium phosphate on top of polymerized silica gel, obtained by AES and Ar-ion milling, are shown in Fig. 12. The calcium phosphate-rich layer extends to a depth of nearly 0.8  $\mu\text{m}$  after only 1 h in rat bone. The silica-rich film is already several micrometers thick. Organic constituents containing C and N are incorporated in the growing calcium phosphate-rich film.

Within 40 min (Fig. 11) the P–O bond-

ing vibration is strong and exhibits a continually decreasing frequency as the calcium phosphate-rich layer builds. At about  $1.5 \pm 0.2$  h, the P–O bending vibration associated with the amorphous calcium phosphate layer is replaced with two P–O modes assigned to crystalline apatite. Concurrent with the onset of apatite crystallization (stage 5 in Table V) is the appearance of a C–O vibrational mode associated with the incorporation of  $\text{CO}_3^{2-}$  in the apatite crystal lattice as described by Kim *et al.*<sup>71</sup> and Le Geros *et al.*<sup>75</sup> The C–O mode decreases in wavenumber as the HCA layer grows. By 10 h the HCA layer has grown to 4  $\mu\text{m}$  in thickness,<sup>67</sup> which is sufficient to dominate the FTIR spectra and mask most of the vibrational modes of the silica-gel layer or the bulk-glass substrate. By 100 h the polycrystalline HCA layer is thick enough to yield X-ray diffraction (XRD) results showing the primary  $26^\circ$  and  $33^\circ$   $2\theta$  peaks with considerable line broadening.<sup>14,76</sup> By 2 weeks the crystalline HCA layer is equivalent to biological apatites grown *in vivo*.<sup>75</sup>

Kokubo<sup>69,77</sup> showed that a calcium phosphate-rich layer is also present at the bonding interface between the polycrystalline apatite and wollastonite-based A/W glass-ceramic and bone. However, the  $\text{SiO}_2$ -rich layer was not present, even though a substantial concentration of soluble Si was lost to solution. Likewise, Kokubo and co-workers<sup>69</sup> showed that the calcium

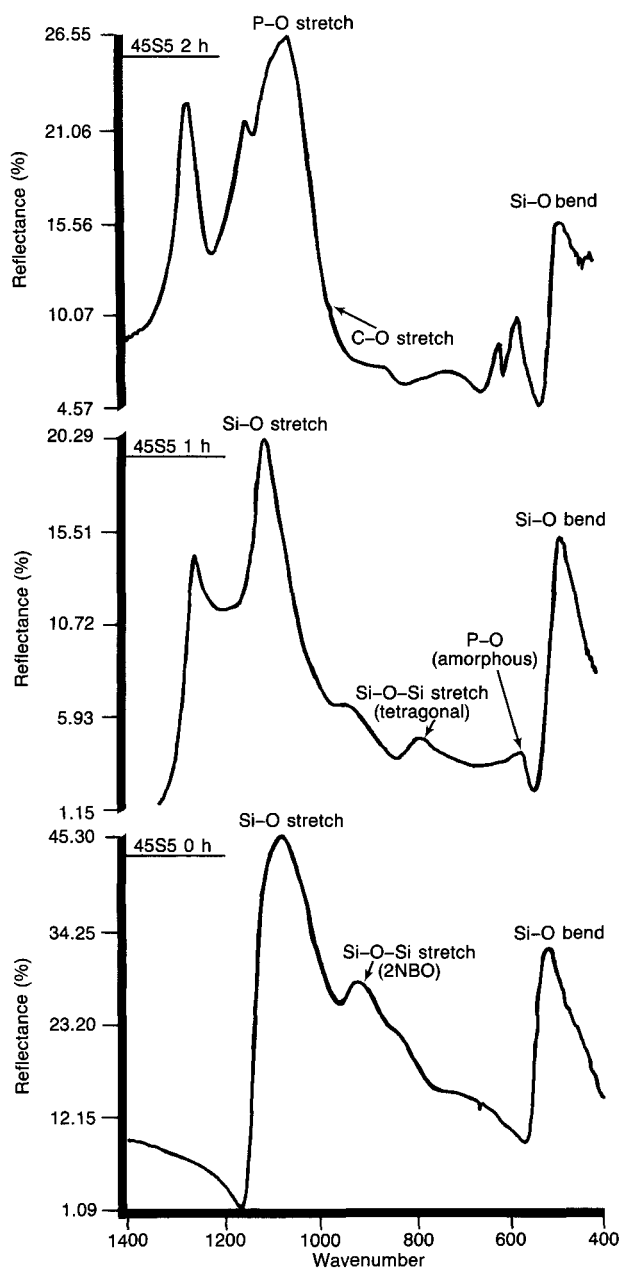


Fig. 10. FTIR spectra of a 45S5 Bioglass® implant after 0, 1, and 2 h in TBS at 37°C. (Diagram courtesy of G. LaTorre.)

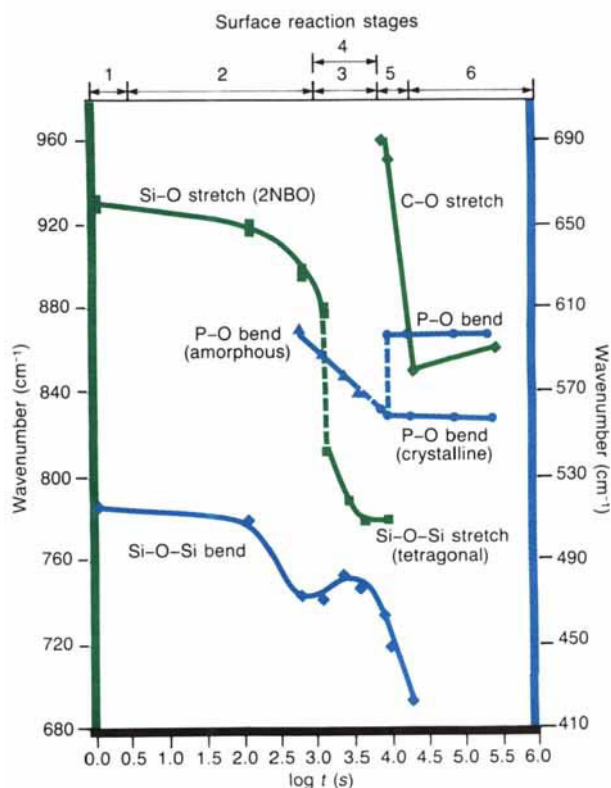


Fig. 11. Time-dependent changes in IR vibrations of the surface of 45S5 Bioglass® implant in a 37°C TBS. (Diagram courtesy of G. LaTorre.)

phosphate-rich layer was present for Ceravital®-type glass-ceramics. Höhland *et al.*<sup>32</sup> reported a calcium phosphate-rich layer at the bone interface with a glass-ceramic composed of phlogopite and apatite crystals. Kokubo and co-workers<sup>77,78</sup> also demonstrated that CaO–SiO<sub>2</sub>-based glasses, without phosphate, formed an apatite layer on their surface when exposed for 2 to 30 d in simulated body fluid that contained only 1.0mM HPO<sub>4</sub><sup>2-</sup>. The CaO–SiO<sub>2</sub> glasses were confirmed to bond to living bone by the surface apatite layer.<sup>77</sup> Previously Ogino, Ohuchi, and the author<sup>67</sup> showed that P<sub>2</sub>O<sub>5</sub>-free Na<sub>2</sub>O–SiO<sub>2</sub> glasses formed an apatite layer on their surface when exposed to an aqueous solution containing calcium and phosphate ions. Recently, Li, Clark, and the author<sup>79</sup> demonstrated that glasses containing primarily SiO<sub>2</sub>, with only 10 mol% of CaO and P<sub>2</sub>O<sub>5</sub> and no Na<sub>2</sub>O formed apatite layers in a tris buffer solution. Earlier, Walker<sup>80</sup> demonstrated that even nearly pure SiO<sub>2</sub> eventually formed a bone bond if the surface had a very high surface area, >400 m<sup>2</sup>/g. Unfortunately, the interface was not analyzed for the presence of an interfacial apatite layer which could have been nucleated on the surface by hydroxylation and/or dissolution of soluble SiO<sub>2</sub>. For years it has been known that synthetic HA implants, which contain no SiO<sub>2</sub> or alkali ions, will bond to bone by forming a new epitaxial apatite phase at the interface,<sup>10,81,82</sup> as discussed in a later section.

Consequently, we conclude that bioactivity occurs only within certain compositional limits and very specific ratios of oxides in the Na<sub>2</sub>O–K<sub>2</sub>O–CaO–MgO–P<sub>2</sub>O<sub>5</sub>–SiO<sub>2</sub> systems; however, the extent of these compositional limits and the physical, chemical, and biochemical reasons for the limits are poorly known at present.

We do know that, for a bond with tissues to occur, a layer of biologically active HCA must form. This is perhaps the only common characteristic of all the known bioactive implant materials. It is the rate of HCA formation (stage 4) and the time for onset of crystallization (stage 5) that varies so greatly. When the rate becomes excessively slow, no bond forms and the material is no longer bioactive. Compositional effects on stages 4 and 5 appear to be critical in controlling bonding, nonbonding, or resorption. Our next step in understanding is to relate the implant surface reactions to in vivo response.

### VIII. Relation of Surface Kinetics to Rate of Bone Bonding

By changing the compositionally controlled reaction kinetics (Table V), the rates of formation of hard tissue at a bioactive implant interface can be al-

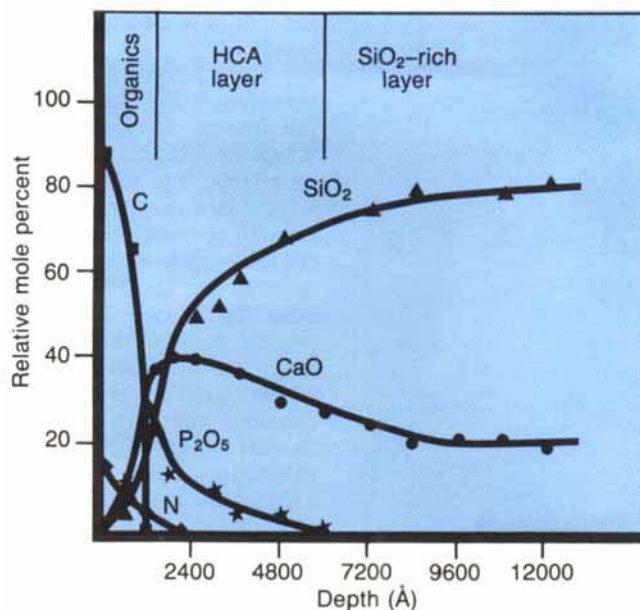


Fig. 12. Bilayer films formed on 45S5 Bioglass® after 1 h in rat bone, in vivo (1 Å = 10<sup>-1</sup> nm) (from Ref. 68).

tered, as shown in Fig. 1. Thus, the relative bioactivity of the material, also shown in Fig. 1, is composition dependent. The level of bioactivity of a specific material can be related<sup>4</sup> to the time for more than 50% of the interface to be bonded ( $t_{0.5bb}$ , where  $I_B = 100/t_{0.5bb}$ ). Gross, Strunz, and colleagues<sup>5,49-52</sup> have shown that the initial concentration of cells present at the interface (stem cells, osteoblasts, chondroblasts, and fibroblasts) varies as a function of the fit of the implant and the condition of the bony defect. Consequently, all bioactive implants require an incubation period before bone proliferates and bonds, which is evident in Fig. 1. The length of the incubation period at which this process occurs varies over a wide range depending on implant composition, which controls the kinetics of the surface reactions (stages 1 to 5 in Table V). For the material to be bioactive and form an interfacial bond, the time of stages 4 and 5 must match the time of biomineralization that normally occurs in vivo. If the surface reactions are too rapid, the implant is resorbable (type 4, Table II). If the reactions are too slow, the implant is not bioactive; i.e., it has a type 1 response.

The compositional dependence of  $I_B$  (Fig. 1) shows that there are  $isoI_B$  contours within the bioactivity boundary, as shown in Fig. 8.<sup>4</sup> The change of  $I_B$  with SiO<sub>2</sub>/(Na<sub>2</sub>O+CaO) ratio is very large as the bioactivity boundary is approached, at 60%–SiO<sub>2</sub>/ $I_B \rightarrow 0$ . Addition of multivalent ions to a bioactive glass or glass-ceramic will serve to shrink the  $isoI_B$  contours. Thus, the  $isoI_B$  contours decrease as the percentage of Al<sub>2</sub>O<sub>3</sub>, Ta<sub>2</sub>O<sub>5</sub>, and ZrO<sub>2</sub> increases in the material. Consequently, the  $isoI_B$



boundary shown in Fig. 8 shows the contamination limit for bioactive glasses and glass-ceramics. If a starting implant composition is near the  $I_B$  boundary, it may take only a few parts per million of multivalent cations to shrink the  $I_B$  boundary to zero and eliminate bioactivity. Also, the sensitivity of fit of a bioactive implant and length of time of immobilization postoperatively depends upon the  $I_B$  value and closeness to the  $I_B=0$  boundary. Implants near the  $I_B$  boundary require more precise surgical fit and longer fixation times before loading. The bioactive phases used in composites must have  $I_B$  values well away from the boundary to start to bond within the 2 to 4 weeks required clinically.

Bioactive implants with intermediate  $I_B$  values do not develop a stable soft-tissue bond: instead the fibrous interface progressively mineralizes to form bone. Consequently, there is a critical  $isoI_B$  boundary beyond which bioactivity is restricted to stable bone bonding. Inside the critical  $isoI_B$  boundary the bioactivity includes both stable bone

and soft-tissue bonding depending on the progenitor stem cells in contact with the implant. This soft-tissue critical  $isoI_B$  limit is shown by the dashed contour in Fig. 8, based on the work of Wilson and Nolletti.<sup>42</sup>

The thickness of the bonding zone between a bioactive implant and bone is proportional to its  $I_B$  value (compare Fig. 1 with Fig. 2). Figure 13 shows an optical micrograph of the interface of 45S5 Bioglass® bonded to bone (rat tibia) after 1 year and an electron microprobe analysis of the interface. The bulk bioactive glass implant (BG), silica-rich layer (S), HCA layer (CA, P), and bone (B) are indicated. Living bone cells (osteocytes labeled O) are at the interface. There is no seam of interfacial fibrous tissue. Even at the electron microscopic level there is almost no unmineralized tissue at the bonding interface, as reviewed by Gross *et al.*<sup>5</sup> and Hench and Clark.<sup>44</sup> The thickness of the bonding region is about 100  $\mu\text{m}$ .

In summary, the reaction stages that appear to be involved in forming the bond of bioactive glasses and bioactive glass-ceramics with tissues are depicted in Fig. 14. The time dependence of the stages shown at the left correspond to implants with high  $I_B$  values. When these stages are lengthened the  $I_B$  values decrease dramatically. If stages 4 and 5 are delayed too long the implant no longer is bioactive. The biological events that occur early in the bonding process are still being established, as discussed by Davies,<sup>83,84</sup> however, the sequence of biological steps appears to be stages 6 to 11 as shown in Fig. 14.

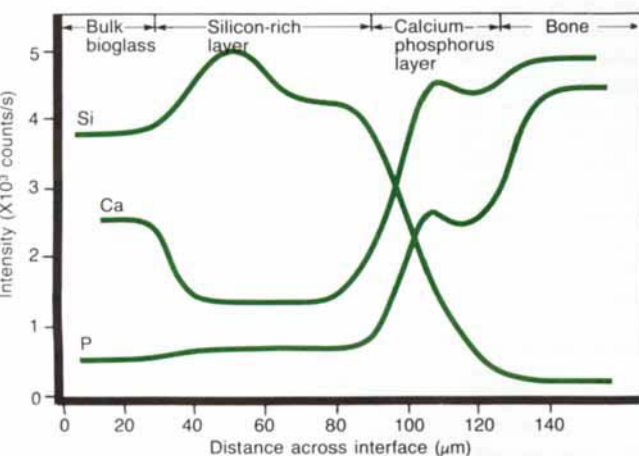
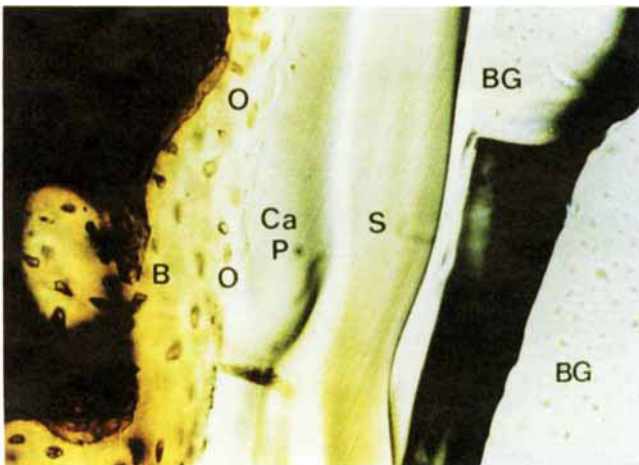


**Fig. 13.** (a) Optical micrograph of a (BG) 45S5 Bioglass® implant bonded to (B) rat bone after 1 year showing (O) osteocytes or bone cells in conjunction with the (Ca-P) HCA layer formed on top of the (S) silica gel (from Ref. 44). (b) Electron microprobe analysis across the implant-bone interface shown in (a) (electron microprobe at 20 kV, 100 nA (specimen current), ~1- $\mu\text{m}$  beam diameter, and 20  $\mu\text{m}/(\text{min} \cdot \text{in.})$  scan rate) (from Ref. 44).

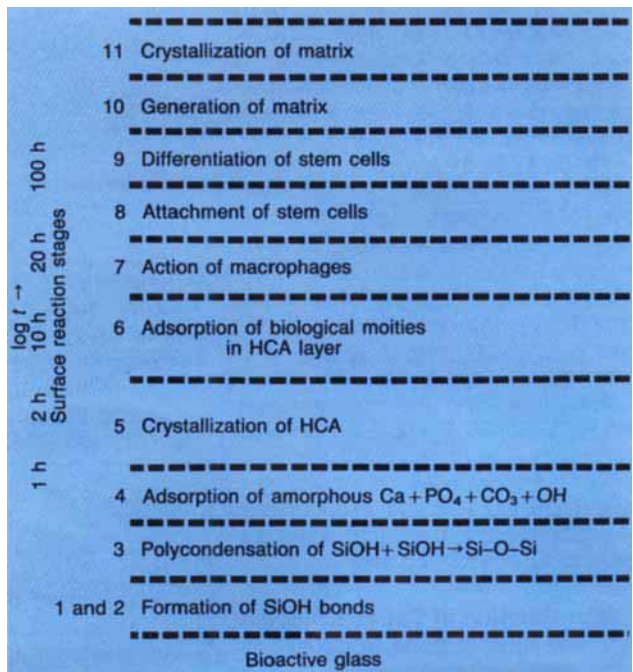


**Fig. 14.** Sequence of interfacial reactions involved in forming a bond between tissue and bioactive ceramics.

The failure strength of a bioactively fixed bond appears to be a nonlinear function of the  $I_B$  value of the implant. Instead, interfacial strength appears to be inversely dependent on the thickness of the bonding zone. For example, 45S5 Bioglass® with a very high  $I_B$  value develops a gel-bonding layer of 100  $\mu\text{m}$  (Fig. 13) which has a relatively low shear strength. In contrast, A/W glass-ceramic, with an intermediate  $I_B$  value has a bonding interface in the range of 10 to 20  $\mu\text{m}$  and a very high resistance to shear (see Fig. 7). Thus, the interfacial bonding strength appears to be optimum for  $I_B$  values of  $\sim 4$ . However, it is important to recognize that the interfacial area for bonding is time dependent, as shown in Fig. 1. Therefore, interfacial strength is time dependent and is a function of morphological factors such as the change in interfacial area with time, progressive mineralization of the interfacial tissues, and a resulting increase of the elastic modulus of the interfacial bond as well as a function of shear strength per unit of bonded area. Few data exist to quantify these variables.

Clinical applications of bioactive glasses and glass-ceramics are reviewed by Gross *et al.*,<sup>5</sup> Yamamuro *et al.*,<sup>41</sup> and Hench and Wilson<sup>30</sup> (see Table VI). The 8-year history of successful use of Ceravital® glass-ceramics and 45S5 Bioglass® implants in middle-ear surgery to replace ossicles damaged by chronic infection, reported by Reck,<sup>85</sup> Merwin,<sup>86</sup> and Douek,<sup>87</sup> are especially encouraging as is the use of A/W glass-ceramic in replacing the iliac crest and in vertebral surgery by Yamamuro.<sup>40,88,89</sup> 45S5 Bioglass® implants have been used successfully for maintenance of the alveolar ridge for denture wearers for up to 7 years<sup>90</sup> with nearly a 90% retention rate, as reported by Stanley *et al.*<sup>90</sup>

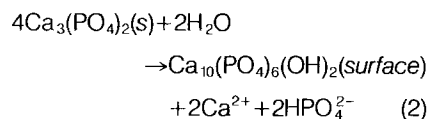
Many patients are profoundly deaf because of loss of the auditory nerve fibers in the cochlea. Research has shown that such patients can still "hear" electronic impulses applied to the cochlea, although at much lower frequency discrimination. These findings have led to the development of an extracochlear electrical implant which delivers electrical signals in real time encoded by a computer to match speech patterns.<sup>91</sup> A team led by Fourcin and Douek in London report<sup>91</sup> successful clinical use of an array of four platinum electrodes, insulated by medical-grade alumina and anchored in the bone with a 45S5 Bioglass® sleeve. The alumina provides mechanical and dielectric stability to the device and the bioactive glass bonds both to the bone and the soft connective tissues as it protrudes through the skin. This hermetic, percutaneous living seal both provides mechanical stability and pre-

vents infection from migrating down the electrodes thereby protecting the patient, who must unplug the electronics at night. Figure 15(a) shows the University of London extracochlear electrode array and its implantation site. Figure 15(b) shows the implant in place in a patient.

### IX. Calcium Phosphate Ceramics

Calcium phosphate-based bioceramics have been in use in medicine and dentistry for nearly 20 years, as reviewed by Hulbert *et al.*,<sup>3</sup> de Groot,<sup>10,13</sup> de Groot and Le Geros,<sup>12</sup> Jarcho,<sup>33</sup> and Williams.<sup>82</sup> Applications include dental implants, percutaneous devices, and use in periodontal treatment, alveolar ridge augmentation, orthopedics, maxillofacial surgery, otolaryngology, and spinal surgery (Table VI). Different phases of calcium phosphate ceramics are used depending upon whether a resorbable or bioactive material is desired.

The stable phases of calcium phosphate ceramics depend considerably upon temperature and the presence of water, either during processing or in the use environment. At body temperature only two calcium phosphates are stable in contact with aqueous media, such as body fluids; at pH < 4.2 the stable phase is  $\text{CaHPO}_4 \cdot 2\text{H}_2\text{O}$  (dicalcium phosphate<sup>9</sup> or brushite,  $\text{C}_2\text{P}$ ), whereas at pH  $\geq 4.2$  the stable phase is  $\text{Ca}_{10}(\text{PO}_4)_6(\text{OH})_2$  (HA). At higher temperatures other phases, such as  $\text{Ca}_3(\text{PO}_4)_2$  ( $\beta$ -tricalcium phosphate,  $\text{C}_3\text{P}$ , or TCP) and  $\text{Ca}_4\text{P}_2\text{O}_9$  (tetracalcium phosphate,  $\text{C}_4\text{P}$ ) are present. The unhydrated high-temperature calcium phosphate phases interact with water, or body fluids, at 37°C to form HA. The HA forms on exposed surfaces of TCP by the following reaction:



Thus, the solubility of a TCP surface approaches the solubility of HA and decreases the pH of the solution which further increases the solubility of TCP and enhances resorption. Williams<sup>82</sup> discusses the importance of the Ca/P ratio in determining solubility and tendency for resorption in the body. The presence of micropores in the sintered material can increase the solubility of these phases.<sup>10-13,33</sup>

Sintering of calcium phosphate ceramics usually occurs in the range of 1000° to 1500°C following compaction of the powder into a desired shape.<sup>33</sup> The phases formed at high temperature depend not only on temperature but also on the partial pressure of water in the sintering atmosphere.

**Table VI. Present Uses of Bioceramics**

Orthopedic load-bearing applications	$\text{Al}_2\text{O}_3$ Stabilized zirconia PE-HA composite
Coatings for chemical bonding (orthopedic, dental, and maxillofacial prosthetics)	HA Bioactive glasses Bioactive glass-ceramics
Dental implants	$\text{Al}_2\text{O}_3$ HA Bioactive glasses
Alveolar ridge augmentations	$\text{Al}_2\text{O}_3$ HA HA-autogenous bone composite HA-PLA composite Bioactive glasses
Otolaryngological	$\text{Al}_2\text{O}_3$ HA Bioactive glasses Bioactive glass-ceramics
Artificial tendon and ligament	PLA-carbon-fiber composite
Artificial heart valves	Pyrolytic carbon coatings
Coatings for tissue ingrowth (cardiovascular, orthopedic, dental, and maxillofacial prosthetics)	$\text{Al}_2\text{O}_3$
Temporary bone space fillers	TCP Calcium and phosphate salts
Periodontal pocket obliteration	HA HA-PLA composite TCP Calcium and phosphate salts Bioactive glasses
Maxillofacial reconstruction	$\text{Al}_2\text{O}_3$ HA HA-PLA composite Bioactive glasses
Percutaneous access devices	Bioactive glass-ceramics Bioactive glasses HA
Orthopedic fixation devices	PLA-carbon fibers PLA-calcium phosphate-based glass fibers
Spinal surgery	Bioactive glass-ceramic HA

\*Also called calcium monophosphate.<sup>82</sup>

With water present, HA can be formed and is a stable phase up to 1360°C, as shown in the phase equilibrium diagram for CaO and P<sub>2</sub>O<sub>5</sub> with 500-mmHg (~66-kPa) partial pressure of water (Fig. 16). Without water, C<sub>4</sub>P and C<sub>3</sub>P are the stable phases.

The temperature range of stability of HA increases with the partial pressure of water as does the rate of phase transitions of C<sub>3</sub>P or C<sub>4</sub>P to HA. Because of kinetics barriers which affect the rates of formation of the stable calcium phosphate phases, it is often difficult to predict the volume fraction of high-temperature phases that are formed during sintering and their relative stability when cooled to room temperature.

Starting powders can be made by mixing into an aqueous solution the appropriate molar ratios of calcium nitrate and ammonium phosphate which

yield a precipitate of stoichiometric HA. The Ca<sup>2+</sup>, PO<sub>4</sub><sup>3-</sup>, and OH<sup>-</sup> ions can be replaced by other ions during processing or in physiological surroundings; e.g., fluorapatite, Ca<sub>10</sub>(PO<sub>4</sub>)<sub>6</sub>(OH)<sub>2-x</sub> where 0 < x < 2 and carbonate apatite, Ca<sub>10</sub>(PO<sub>4</sub>)<sub>6</sub>(OH)<sub>2-2x</sub>(CO<sub>3</sub>)<sub>x</sub> or Ca<sub>10-x+y</sub>(PO<sub>4</sub>)<sub>6-x</sub>(OH)<sub>2-x-2y</sub> where 0 < x < 2 and 0 < y < 0.5x can be formed. Fluorapatite is found in dental enamel and HCA is present in bone. For a discussion of the structure of these complex crystals see Ref. 81 (Le Geros).

The mechanical behavior of calcium phosphate ceramics strongly influences their application as implants.<sup>12</sup> Tensile and compressive strength and fatigue resistance depend on the total volume of porosity. Porosity can be in the form of micropores (<1 μm in diameter, due to incomplete sintering) or macropores (>100 μm in diameter, created to permit bone growth). The dependence of compressive strength (σ<sub>c</sub>) and total pore volume (V<sub>p</sub>) is described by de Groot *et al.*<sup>13</sup> as

$$\sigma_c = 700 \exp(-5V_p) \text{ MPa} \quad (3)$$

where V<sub>p</sub> is in the range 0 to 0.5. Tensile strength (σ<sub>t</sub>) depends greatly on the volume fraction of microporosity (V<sub>m</sub>):

$$\sigma_t = 220 \exp(-20V_m) \text{ MPa} \quad (4)$$

The Weibull factor (n) of HA implants is low in physiological solutions (n=12), which indicates low reliability under

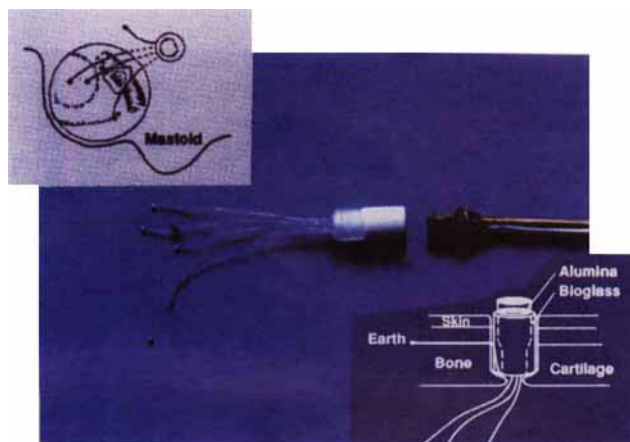


**Fig. 15.** (a) Extracochlear electrical implant for the profound deaf showing (center) electrode array, (upper left) implantation site, and (lower right) schematic of the components. (b) Implant in patient's ear, with electronics disconnected. (Photographs courtesy E. Douek.)

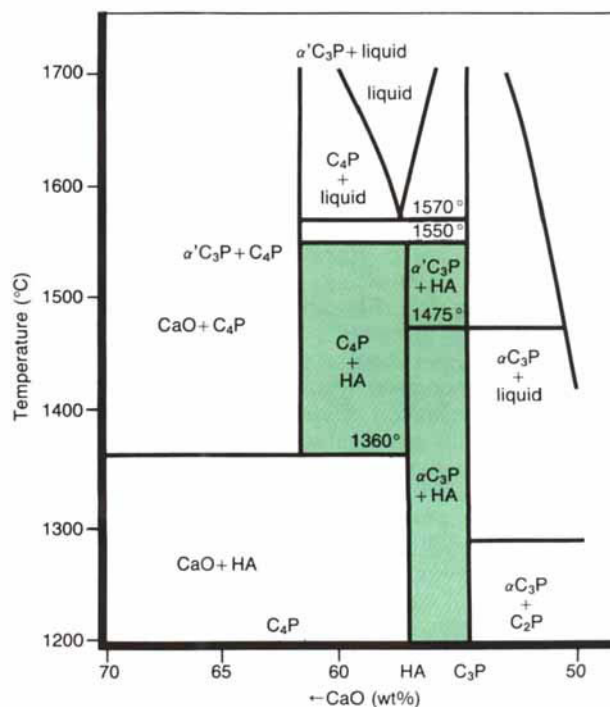


**Fig. 16.** Calcium phosphate phase equilibrium diagram with 500-mmHg (~66-kPa) partial pressure of water. Shaded area is processing range to yield HA-containing implants. (Diagram based upon Ref. 13.)



tensile loads. Consequently, in clinical practice calcium phosphate bioceramics should be used as (1) powders, (2) small, unloaded implants such as in the middle ear, (3) dental implants with reinforcing metal posts, (4) coatings on metal implants, (5) low-loaded porous implants where bone growth acts as a reinforcing phase, or (6) the bioactive phase in a polymer-bioactive ceramic composite.

The bonding mechanisms of dense HA implants appear to be very different from those described earlier for bioactive glasses. Evidence for the bonding process for HA implants is reviewed by Jarcho.<sup>33</sup> A cellular bone matrix from differentiated osteoblasts appears at the surface, producing a narrow amorphous electron-dense band only 3 to 5  $\mu\text{m}$  wide. Between this area and the cells, collagen bundles are seen. Bone mineral crystals have been identified in this otherwise amorphous area.<sup>92</sup> As the site matures, the bonding zone shrinks to a depth of only 0.05 to 0.2  $\mu\text{m}$ . The result is normal bone attached through a thin epitaxial bonding layer to the bulk implant.<sup>92</sup> Ogiso *et al.*<sup>93,94</sup> have shown, through transmission electron microscopy (TEM) lattice image analysis of dense HA bone interfaces, an almost perfect epitaxial alignment of the growing bone crystallites with the apatite crystals in the implant (Fig. 17).

A consequence of this ultrathin bonding zone is a very high gradient in elastic modulus at the bonding interface between HA and bone. This is one of the major differences between the bioactive apatites and the bioactive glasses and glass-ceramics, as illustrated in Fig. 2. The implications of this difference on the interfacial response of the implant to applied stress and bone vitality is discussed in Ref. 1 (Ch. 14). The significance of this difference clinically is as yet unknown.

Potentially, one of the most important applications of sintered, dense HA implants is as percutaneous access assist devices (PAD)<sup>95</sup> for continuous ambulatory peritoneal dialysis (CAPD) patients. There are hundreds of thousands of patients worldwide who undergo renal dialysis and could benefit from CAPD, which would decrease their dependency on the resources required for conventional hemodialysis.<sup>96</sup> However, a severe limitation on CAPD is the incidence of peritonitis, up to 1.5 incidents per year per patient, usually caused by invasion of bacteria along the wall of the inserted peritoneal catheter. Catheters used, now made of silicone rubber, do not form a completely sealed junction with the skin or subcutaneous tissues and thereby provide a pathway for infection to occur.

Aoki and colleagues<sup>95,96</sup> have shown



**Fig. 17.** TEM micrograph using lattice imaging to show epitaxial bonding between (bottom) HA implants and (top) the HA phase of bone. (Photograph courtesy of M. Ogiso.)



**Fig. 18.** Stable HA implant in forearm of a volunteer 6 years after implantation. (Photograph courtesy of H. Aoki.)

that a dense, sintered HA implant, used in contact with skin and subcutaneous tissues, provides a stable seal and has prevented downgrowth of epidermis and infiltration of cells, common characteristics of glassy carbon or silicone rubber percutaneous leads. Figure 18 shows a HA implant in the arm of a volunteer after 6 years without any serious infection. X-ray computer tomography of the forearm showed no calcification of the soft tissues around the skin button.<sup>97</sup>

Two patients suffering from end-stage renal disease developed arterio-venous fistulas after 10 months and 12 years hemodialysis, and therefore, could not continue treatment. After implantation of an HA PAD and CAPD treatment, they have remained well for more than 2 years,<sup>96</sup> indicating the value of this application of bioactive ceramics.

## X. Composites

One of the primary restrictions on clinical use of bioceramics is the uncertain lifetime under the complex stress

**Table VII. Number of Centers Represented at World Biomaterials Congress**

Country	Year		
	1980	1984	1988
United States	2	6	7
FRG	2	1	2
Netherlands	1	1	2
Japan	1	3	14
Italy		1	2
United Kingdom			2
France			3
Finland			1
Belgium			1
DRG			1
Total	6	12	35

states, slow crack growth, and cyclic fatigue that arise in many clinical applications. Two creative approaches to these mechanical limitations are use of bioactive ceramics as coatings or in composites. Much of the rapid growth in the field of bioactive ceramics, summarized in Table VII is due to development of various composite and coating systems, as reviewed by Doyle,<sup>99</sup> Ducheyne and McGuckin,<sup>100</sup> and Soletz.<sup>101</sup> Many papers in Refs. 25 and 41 also discuss these topics. Tables VIII and IX show that composites and coatings involve all three types of biomaterials—nearly inert, resorbable, and bioactive—and reflect differing rationales in their development. In most

cases the goal is to increase flexural strength and strain to failure and decrease elastic modulus.

Bonfield<sup>102</sup> argues that analogous implant materials with similar mechanical properties should be the goal when bone is to be replaced. Because of the anisotropic deformation and fracture characteristics of cortical bone, which is itself a composite of compliant collagen fibrils and brittle HCA crystals, the Young's modulus ( $E$ ) varies between  $\sim 7$  to 25 GPa, the critical stress intensity ranges from  $\sim 2$  to 12 MPa $\cdot$ m<sup>1/2</sup>, and the critical strain intensity increases from as low as  $\sim 600$  J $\cdot$ m<sup>-2</sup> to as much as 5000 J $\cdot$ m<sup>-2</sup>, depending on orientation, age, and test condition.<sup>103</sup> In contrast, most bioceramics are much stiffer than bone and many exhibit poor fracture toughness (Table III). Consequently, one approach to achieve properties analogous to bone is to stiffen a compliant biocompatible synthetic polymer, such as PE, with a higher modulus ceramic second phase, such as HA powder.<sup>102</sup> The effect is to increase Young's modulus from 1 to 8 GPa and to decrease the strain to failure from  $>90\%$  to 3% (Fig. 19) as the volume fraction of HA increases to 0.5. The transition from ductile to brittle behavior occurs between 0.4 and 0.45 volume fraction HA. Bonfield<sup>102</sup> reported that the ultimate tensile strength of the composite remained within the range of 22 to 26 MPa. At 0.45 volume fraction HA, the  $K_{IC}$  value was  $2.9 \pm 0.3$  MPa $\cdot$ m<sup>1/2</sup>, whereas at  $<0.4$  volume fraction HA the fracture toughness was considerably greater, because of the ductile deformation associated with crack propagation. Thus, the mechanical properties of the PE-HA composite are close to or superior to those of bone.

The bioactive phase is exposed by machining the surface of the composite. Implant tests of the PE+0.4HA composites have demonstrated development of bone bonding between the natural hard tissue and the synthetic implant.<sup>104</sup> An application of the PE-HA composite currently in test in London is as a medullary sleeve for fixation of the stem of femoral head replacements, where the bonding of the composite to bone should prevent stress shielding because of its match of Young's modulus with the bone. Figure 20 depicts such a device.

Another promising approach toward achieving high toughness, ductility, and a Young's modulus matching that of bone was developed by Ducheyne and the author.<sup>107</sup> This composite uses sintered 316L stainless steel of 50-, 100-, or 200- $\mu$ m diameter or titanium fibers, which provide an interconnected fibrous matrix which is then impregnated with molten 45S5 Bioglass®. After the composite is cooled and annealed, a very strong and tough material results, with

**Table VIII. Bioceramic Composites**

Matrix	Reinforcing phase*	Reference
Type 1: Nearly inert composites		
Polysulfone	Carbon fiber	99, 101
Polyethylene	Carbon fiber	99, 101
Poly(methyl methacrylate)	Carbon fiber	
Carbon	Carbon fiber	99
Carbon	SiC	101
Epoxy resin	Alumina/stainless steel	101
Type 2: Porous ingrowth composites		
Coral HA goniopora	DL polylactic acid	105
Type 3: Bioactive composites		
Bioglass®	Stainless-steel fibers	100, 101
Bioglass®	Titanium fiber	100, 101
Collagen	HA	99, 101
Polyethylene	HA	102, 101
Poly(methyl methacrylate)	Phosphate-Silicate-Apatite glass fiber	99, 101
Polymer	Phosphate glass	99, 101
HA/collagen	Gelatin-resorcinol-formaldehyde	99
A/W glass-ceramic	Transformation-toughened ZrO <sub>2</sub>	106
Type 4: Resorbable composites		
PLA/PGA	PLA/PGA fibers	99, 101
Polyhydroxybuturate	HA	99, 101
PLA/PGA	HA	99, 101

\*DL is dextra levorotatory (left handed).

**Table IX. Bioceramic Coatings**

Substrate	Coating	Reference
316L stainless steel	Pyrolytic carbon	Bockros <sup>110</sup>
316L stainless steel	45S5 Bioglass®	Hench <sup>57</sup>
316L stainless steel	$\alpha$ -Al <sub>2</sub> O <sub>3</sub> -HA-TiN	Hayashi <sup>25</sup>
316L stainless steel	HA	Munting <sup>25</sup>
316L stainless steel	SE51(45S5) Bioglass®	Ito <sup>41</sup>
Co-Cr alloy	45S5 Bioglass® and 52S4.6 Bioglass®	Lacefield <sup>119</sup>
Co-Cr alloy	HA	Munting <sup>25</sup>
Ti-6Al-4V alloy	45S5 Bioglass®	West <sup>41</sup>
Ti-6Al-4V alloy	HA/ABS Glass*	Maruns <sup>25</sup>
Ti-6Al-4V alloy	HA	Ducheyne <sup>25</sup>
Ti-6Al-4V alloy	TCP	Cook <sup>114</sup>
		Lacefield <sup>25</sup> , Chae <sup>25</sup>
Ti-6Al-4V alloy	HA	Hamada <sup>25</sup>
Ti-6Al-4V alloy	Al <sub>2</sub> O <sub>3</sub>	Hamada <sup>25</sup>
Ti-6Al-4V alloy+porous beads	HA	Oonishi <sup>25</sup>
Ti-6Al-4V alloy	TiO <sub>2</sub> -HA	Hayashi <sup>25</sup>
Ti-6Al-4V alloy	HA, TRP, TCP	de Groot <sup>25</sup>
Ti-6Al-4V alloy+Ti powder	HA	Ducheyne <sup>25</sup>
Ti-6Al-4V alloy	HA	Kay <sup>25</sup>
Alumina	45S5 Bioglass®	Greenspan <sup>46</sup>

\*ABS is alkali borosilicate glass.

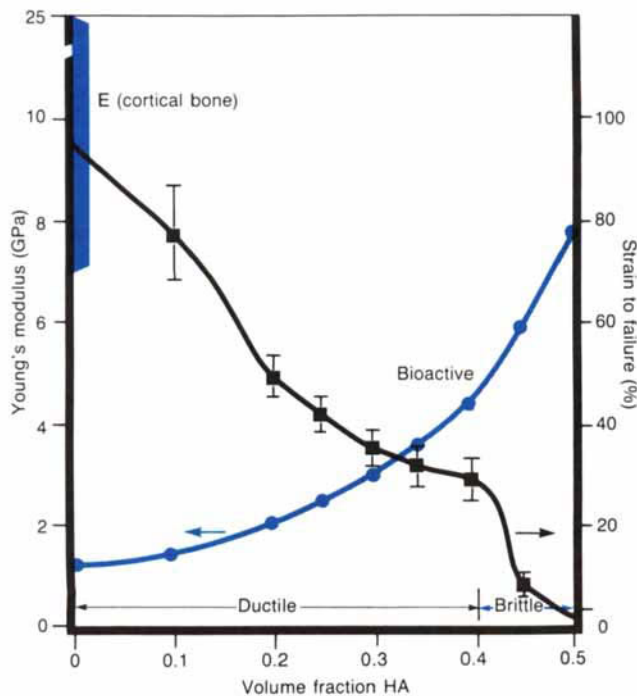


**Fig. 19.** Effect of HA on Young's modulus and strain to failure of a PE-HA composite. (Based upon data of Ref. 102.)



**Fig. 20.** PE-HA composite used as a sleeve for the stem of a total hip implant. (Photograph courtesy of W. Bonfield.)

metal-to-glass volume ratios between 4/6 to 6/4. Strength enhancements of up to 340 MPa are obtained in bending with substantial ductility of up to 10% elongation, as shown by the set of bend-test bars in Fig. 21, which bent 90° without fracturing. When an outer coating of Bioglass® is maintained, the composite implants bond to bone tissue and perform a load-carrying function.<sup>108</sup>

The strongest of the bioactive ceramic composites is composed of A/W glass-ceramic containing a dispersion of tetragonal zirconia, developed by Kasuga *et al.*<sup>106</sup> Volume fractions of 0.5 zirconia lead to bend strength values of 703 MPa and  $K_{IC}$  values of 4 MPa·m<sup>1/2</sup> and also formed HA on their surface under in vitro test conditions. These results, with other composite systems listed in Table VIII, indicate the great potential of bioactive and resorbable bioceramics with good mechanical behavior for a wide variety of clinical applications. As yet, however, very little data exist on the environmental sensitivity and fatigue life of these composite systems under physiological loads and environments. Until these data are acquired caution must be exercised when using such materials clinically, other than in highly controlled trials.

## XI. Coatings

### (1) Carbon

Bokros<sup>109</sup> applied, in 1967, for a patent describing the medical use of pyrolytic carbon coatings on metal substrates. The coatings were used in

heart surgery soon thereafter.<sup>110</sup> The first time the low-temperature isotropic (LTI) carbon coatings were used in humans was as a prosthetic heart valve by DeBakey in 1969.<sup>110</sup>

Almost all commonly used prosthetic heart valves today have LTI carbon coatings for the orifice and/or occluder (Fig. 22) because of their excellent resistance to blood clot formation and long fatigue life.<sup>111</sup> More than 600 000 lives have been prolonged through the use of this bioceramic in heart valves.<sup>113</sup>

Three types of carbon are used in biomedical devices: the LTI variety of pyrolytic carbon, glassy (vitreous) carbon, and the ultralow-temperature isotropic (ULTI) form of vapor-deposited carbon.<sup>112,113</sup> These carbon materials are integral and monolithic materials (glassy carbon and LTI carbon) or impermeable thin coatings (ULTI carbon). These three forms do not suffer from the integrity problems typical of other available carbon materials. With the exception of the LTI carbons codeposited with silicon, all the carbon materials in clinical use are pure elemental carbon. Up to 20 wt% silicon has been added to LTI carbon without significantly affecting the biocompatibility of the material. The composition, structure, and fabrication of the three clinically relevant carbons are unique when compared with the more common, naturally occurring form of carbon (i.e., graphite) and other industrial forms produced from pure elemental carbon.

The LTI, ULTI, and glassy carbons are subcrystalline forms and represent

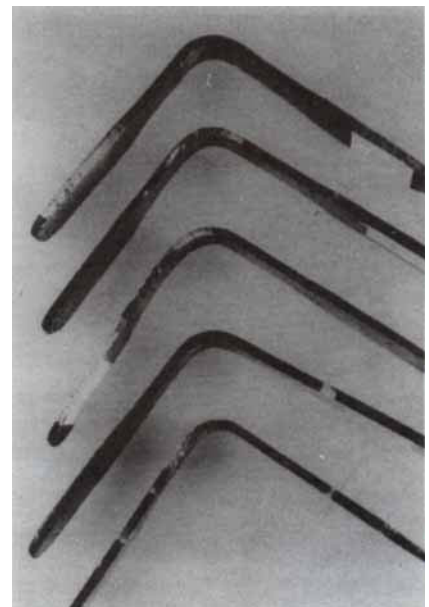


**Fig. 21.** 45S5 Bioglass® composite reinforced with 60% of 100- $\mu$ m 316L stainless-steel fibers tested in bending. Note a bend angle of  $>90^\circ$  is obtained without failure.<sup>107</sup> (Photograph courtesy of P. Ducheyne.)



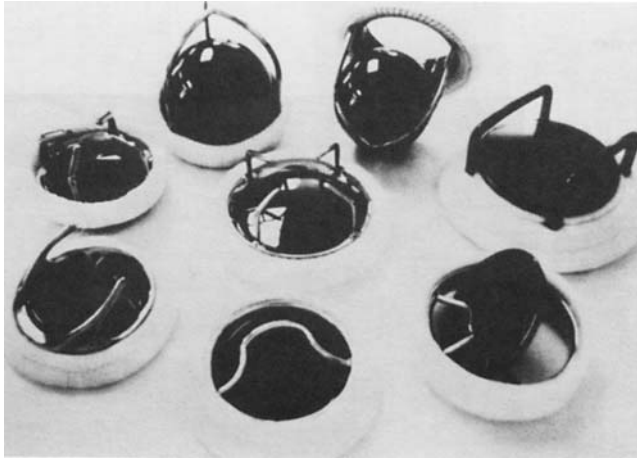


**Fig. 22.** LIT pyrolytic carbon-coated heart valves. (Photograph courtesy of J. Bokros.)

a lower degree of crystal perfection. There is no order between the layers such as there is in graphite; therefore, the crystal structure of these carbons is two dimensional. Such a structure, called turbostratic, has densities between about 1400 and 2100  $\text{kg} \cdot \text{m}^{-3}$ . High-density LTI carbons are the strongest bulk forms of carbon and their strength can further be increased by adding silicon. ULTI carbon can also be produced with high densities and strengths, but it is available only as a thin coating (0.1 to 1.0  $\mu\text{m}$ ) of pure carbon. Glassy carbon is inherently a low-density material and, as such, is weak. Its strength cannot be increased through processing. Processing of all three types of medical carbons are discussed in Ref. 113 (Haubold *et al.*).

The mechanical properties of the various carbons are intimately related to their microstructures. In an isotropic carbon, it is possible to generate materials with low elastic moduli (20 GPa) and high flexural strength (275 to 620 MPa). There are many benefits as a result of this combination of properties; e.g., large strains ( $\sim 2\%$ ) are possible without fracture. The turbostratic carbons are very tough when compared with ceramics such as aluminum oxide. The energy to fracture for LTI carbon is approximately  $5.5 \text{ MJ} \cdot \text{m}^{-3}$ , compared with  $0.18 \text{ MJ} \cdot \text{m}^{-3}$  for aluminum oxide; i.e., the carbon is approximately 25 times as tough. The strain to fracture for the vapor-deposited carbons is greater than 5.0%, making it feasible to coat highly flexible polymeric materials such as PE, polyesters, and nylon without fear of fracturing the coating when the substrate is flexed.

The turbostratic carbon materials have extremely good wear resistance, some of which can be attributed to their toughness, i.e., their capacity to sustain large local elastic strains under

concentrated or point loading without galling or incurring surface damage. The bond strength of the ULTI carbon to stainless steel and to Ti-6Al-4V exceeds 70 MPa as measured with a thin-film adhesion tester. This excellent bond is, in part, achieved through the formation of interfacial carbides. The ULTI carbon coating generally has a lower bond strength with materials that do not form carbides.

Another unique characteristic of the turbostratic carbons is that they do not fail in fatigue. The ultimate strength of turbostratic carbon, as opposed to metals, does not degrade with cyclical loading. The fatigue strength of these carbon structures is equal to the single-cycle fracture strength. It appears that, unlike other crystalline solids, these forms of carbon do not contain mobile defects, which at normal temperatures can move and provide a mechanism for the initiation of a fatigue crack.

The more important known properties of the turbostratic carbons are listed in Ref. 113.

Carbon surfaces are not only thromboresistant, but also appear to be compatible with the cellular elements of blood; they do not influence plasma proteins or alter the activity of plasma enzymes. One of the proposed explanations for the blood compatibility of these materials is that they adsorb blood proteins on their surface without altering them.

Reference 113 summarizes the uses of glassy, LTI, and ULTI carbons in various medical areas.

## (2) Hydroxyapatite

A second bioceramic coating which has reached a significant level of clinical application is the use of HA as a coating on porous metal surfaces for fixation of orthopedic prostheses. This approach combines types 2 and 3 methods of fixation (Table II) and originates from the observations of Ducheyne and colleagues,<sup>9</sup> in 1980, that HA powder in the pores of a porous, coated-metal implant would significantly affect the rate and vitality of bone ingrowth into the pores. A large number of investigators have explored various means of applying the HA coating, as discussed in Refs. 3, 5, 12, 25, 41, and 101, with plasma spray coating generally being preferred. There is a substantial enhancement of the early stage interfacial bond strength of implants with a plasma-sprayed HA coating when compared with porous metals without the coating, as illustrated in Fig. 23, from Cook.<sup>114</sup> However, long-term animal studies and clinical trials of load-bearing dental and orthopedic prostheses suggest that the HA coatings may degrade or come off, and the clinical consequences are still being debated.<sup>84</sup>

## XII. Resorbable Calcium Phosphates

Resorption or biodegradation of calcium phosphate ceramics is caused by (1) physiochemical dissolution, which depends on the solubility product of the material and local pH of its environment (New surface phases may be formed, e.g., amorphous calcium phosphate, dicalcium phosphate dihydrate, octacalcium phosphate ( $\text{Ca}_8(\text{PO}_4)_3\text{H} \cdot 3\text{H}_2\text{O}$ ), and anionic substituted HA.); (2) physical disintegration into small particles due to preferential chemical attack of grain boundaries; and (3) biological factors, such as phagocytosis, which causes a decrease in local pH.<sup>12</sup>

All calcium phosphate ceramics biodegrade to varying degrees in the following order:  $\alpha$ -TCP >  $\beta$ -TCP > HA.

The rate of biodegradation increases as (1) surface area increases (powders > porous solid > dense solid), (2) crystallinity decreases, (3) crystal perfection decreases, (4) crystal and grain size decrease, and (5) ionic substitutions of  $\text{CO}_3^{2-}$ ,  $\text{Mg}^{2+}$ ,  $\text{Sr}^{2+}$  in HA take place. Factors which result in a decreasing rate of biodegradation include (1) F-substitution in HA, (2)  $\text{Mg}^{2+}$  substitution in  $\beta$ -TCP, and (3) decreasing  $\beta$ -TCP/HA ratios in biphasic calcium phosphates. Because of these variables it is necessary to control the microstructure and phase state of a resorbable calcium phosphate bio-ceramic in addition to achieving precise compositional control to produce a given rate of resorption in the body. As yet, there are few data on the kinetics of these reactions and the variables influencing the kinetics.

## XIII. Therapeutic Applications

A significant problem in the radiation treatment of cancer is the serious systemic side effects. Localization of the radiation at the site of the tumor decreases the radiation dosage required to kill the cancer cells and thereby minimizes side-effect toxicities. An innovative approach to the localized delivery of radioactive yttrium-90 ( $^{90}\text{Y}$ ) to treat liver cancer has been developed by Day<sup>114</sup> at the University of Missouri-Rolla using glass microspheres. A yttria-aluminosilicate glass, containing  $^{89}\text{Y}$  is made in the form of 25- $\mu\text{m}$  microspheres. Prior to use in hepatic arterial infusion therapy, the microspheres are bombarded by neutrons which creates  $^{90}\text{Y}$ , a radioactive isotope which is a short half-life (64 h), short-range (2.5 to 3 mm in the liver)  $\beta$  emitter. The microspheres are injected through a catheter placed in an artery, and the blood stream carries them to the liver where a high proportion goes to the cancerous part because of the ~3 times increased blood supply. A localized dosage of up to 15000 rd can

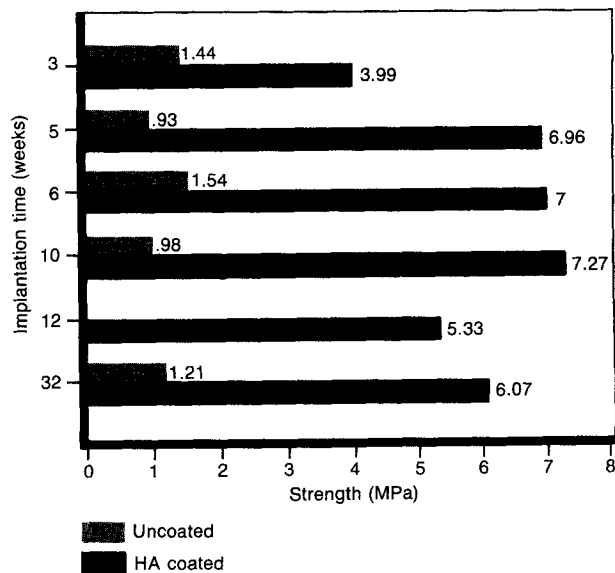


Fig. 23. Comparison of interfacial bond strength of porous titanium with and without plasma-sprayed HA coatings. (Photograph courtesy of S. Cook.)

be delivered in this manner, whereas a maximum of 3000 rd of external radiation can be tolerated by the patient. In a clinical trial in Canada, Boos *et al.*<sup>115</sup> report response for 35 of 46 patients with carcinoma of the liver: complete remission of 1, partial remission of 6, and stability of the disease of 24, with a mean survival of 16.1 months for the responders versus only 8.8 months for nonresponders.

Day<sup>116</sup> reports that the glass-microsphere radiation delivery vehicle can be modified with different radioactive isotopes to achieve various ranges and is being tested preclinically for treatment of kidney cancer and arthritis.

Another approach to cancer treatment using bioceramics is under development by Yamamuro in Kyoto, Japan.<sup>117</sup> Ohura *et al.*<sup>117</sup> have incorporated 40 wt%  $\text{Fe}_2\text{O}_3$  in a bioactive glass-ceramic composed of  $\text{CaO-SiO}_2\text{-B}_2\text{O}_3\text{-P}_2\text{O}_5$ . The magnetite phase produces a high-saturation magnetization which can be used to generate localized heating at an implant site. Temperatures of  $>42^\circ\text{C}$  can be generated in bone, sufficient to kill tumor cells, by applying a 300-Oe, 100-Hz magnetic field. The wollastonite phase which grows during crystallization provides bonding of the granules to bone. Preclinical tests are underway.

Still another therapeutic application of bioceramics is delivery of various steroid hormones from aluminum calcium phosphate porous ceramics.<sup>118</sup> The advantage of this method is sustained delivery of a potentially toxic substance over long periods of time, again inhibiting systemic side effects

due to large dosages. Details of the processing, delivery rates, and many chemical and biological tests are given by Benghussi and Bajpai.<sup>11b</sup>

#### IV. Summary

Bioceramics has evolved to become an integral and vital segment of our modern health-care delivery system. The full potential is only beginning to be recognized. In the years to come the composition, microstructure, and molecular surface chemistry of various types of bioceramics will be tailored to match the specific biological and metabolic requirements of tissues or disease states. This "molecular-based pharmaceutical" approach to the design of bioceramics should couple with the growth of genetic engineering, sensor technology, and information processing, resulting in a range of products and applications not even imagined at present, but potentially beneficial to millions of people annually.

However, at present there is a critical need for standard test methods to determine the long-term lifetime performance of bioceramics under realistic physiological loads. Too many materials are introduced into clinical use without proof tests or lifetime prediction tests. Seldom are interinstitutional studies conducted to determine the reliability of biomechanical performance. Standards do not presently exist for bioactive ceramics or coatings, although the American Society for Testing and Materials (ASTM) F-4 Committee on Medical and Surgical Materials and Devices has a Subcommittee on Ceramic Materials (J. Lemons, Chair) with a goal of achieving standards for bioactive glasses and glass-ceramics (D. Greenspan), hydroxyapatite (H. Hahn), single-crystal and polycrystalline alumina (H. Jung), and ceramic coatings (J. Kay). Standardization of test methods also needs to be established. At present, there is no way to compare interfacial bonding strength data for the materials listed in Tables IV, VIII, or IX. Likewise, there is no basis to compare fatigue life for any of these materials or establishing the relative importance of grain-boundary attack or slow crack growth under standardized conditions. We must correct these deficiencies within this decade because there is a rapidly growing number of failures of load-bearing metallic prostheses with poly(methyl methacrylate) (PMMA) cement fixation. The lifetime of cemented devices is often less than the lifetime of a patient. Therefore, revision surgery is required with great trauma to the patient and great expense to our health-care system. Bioceramics offer one of the few alternatives for solving this problem. However, it is our responsibility to assure that long-term reliability of bioceramics

is proved before clinical use is expanded.

**Acknowledgments:** The author acknowledges the long-term collaboration with June Wilson-Hench, wife and coresearcher, who helped in proofing; Alice Holt for manuscript preparation; and Professor Werner Lutze for a critical review.

#### References

- <sup>1</sup>L. L. Hench and E. C. Ethridge, *Biomaterials: An Interfacial Approach*. Academic Press, New York, 1982.
- <sup>2</sup>J. D. Preston, "Properties in Dental Ceramics"; in *Proceedings of the IVth International Symposium on Dental Materials*. Quintessa Publishing, Chicago, IL, 1988.
- <sup>3</sup>S. F. Hulbert, J. C. Bokros, L. L. Hench, J. Wilson, and G. Heimke, "Ceramics in Clinical Applications: Past, Present, and Future"; pp. 189–213 in *High Tech Ceramics*. Edited by P. Vincenzini. Elsevier, Amsterdam, Netherlands, 1987.
- <sup>4</sup>L. L. Hench, "Bioactive Ceramics"; p. 54 in *Bioceramics: Material Characteristics Versus In Vivo Behavior*, Vol. 523. Edited by P. Ducheyne and J. Lemons. Annals of New York Academy of Sciences, New York, 1988.
- <sup>5</sup>U. Gross, R. Kinne, H. J. Schmitz, and V. Strunz, "The Response of Bone to Surface Active Glass/Glass-Ceramics," *CRC Crit. Rev. Biocompat.*, **4**, 2 (1988).
- <sup>6</sup>P. Christel, A. Meunier, J. M. Dorlot, J. M. Crolet, J. Witvolet, L. Sedel, and P. M. Boutin, "Biomechanical Compatibility and Design of Ceramic Implants for Orthopedic Surgery"; p. 234 in *Bioceramics: Material Characteristics Versus In Vivo Behavior*, Vol. 523. Edited by P. Ducheyne and J. Lemons. Annals of New York Academy of Sciences, New York, 1988.
- <sup>7</sup>L. L. Hench, "Cementless Fixation"; p. 23 in *Biomaterials and Clinical Applications*. Edited by A. Pizzoferrato, P. G. Marchetti, A. Ravaglioli, and A. J. C. Lee. Elsevier, Amsterdam, Netherlands, 1987.
- <sup>8</sup>J. Black, "Systemic Effects of Biomaterials," *Biomaterials*, **5**, 11 (1984).
- <sup>9</sup>P. Ducheyne, L. L. Hench, A. Kagan, M. Martens, A. Bursens, and J. C. Muller, "The Effect of Hydroxyapatite Impregnation of Skeletal Bonding of Porous Coated Implants," *J. Biomed. Mater. Res.*, **14**, 225 (1980).
- <sup>10</sup>K. de Groot, *Bioceramics of Calcium Phosphate*; pp. 1–32. CRC Press, Boca Raton, FL, 1983.
- <sup>11</sup>K. de Groot, "Effect of Porosity and Physicochemical Properties on the Stability, Resorption, and Strength of Calcium Phosphate Ceramics"; in *Bioceramics: Material Characteristics Versus In Vivo Behavior*, Vol. 523. Edited by P. Ducheyne and J. Lemons. Annals of New York Academy of Sciences, New York, 1988.
- <sup>12</sup>K. de Groot and R. Le Geros, "Significance of Porosity and Physical Chemistry of Calcium Phosphate Ceramics"; pp. 268–77 in *Bioceramics: Material Characteristics Versus In Vivo Behavior*, Vol. 523. Edited by P. Ducheyne and J. Lemons. Annals of New York Academy of Sciences, New York, 1988.
- <sup>13</sup>K. de Groot, C. P. A. T. Klein, J. G. C. Wolke, and J. de Bleck-Hogervorst, "Chemistry of Calcium Phosphate Bioceramics"; pp. 3–15 in *Handbook of Bioactive Ceramics*, Vol. II, Calcium Phosphate and Hydroxylapatite Ceramics. Edited by T. Yamamuro, L. L. Hench, and J. Wilson. CRC Press, Boca Raton, FL, 1990.
- <sup>14</sup>L. L. Hench, R. J. Splinter, W. C. Allen, and T. K. Greenlee, Jr., "Bonding Mechanisms at the Interface of Ceramic Prosthetic Materials," *J. Biomed. Mater. Res.*, **2** {1} 117–41 (1972).



- <sup>15</sup>P. Griss and G. Heimke, "Five-Years Experience with Ceramic-Metal Composite Hip Endoprostheses." *Arch. Orthop. Traumat. Surg.*, **98**, 157-65 (1981).
- <sup>16</sup>P.M. Boutin, "A View of 15-Years Results Using the Alumina-Alumina Hip Joint Protheses"; p. 297 in *Ceramics in Clinical Applications*. Edited by P. Vincenzini. Elsevier, New York, 1987.
- <sup>17</sup>H. Oonishi, N. Okabe, T. Hamaguchi, and T. Nabeshima, *Orthopedic Ceramic Implants*, Vol. 1; p. 157 Japanese Society of Orthopaedic Ceramic Implants, Osaka, Japan, 1981.
- <sup>18</sup>H. Plenck, "Biocompatibility of Ceramics in Joint Protheses"; pp. 269-95 in *Biocompatibility of Orthopedic Implants*, Vol. 1. CRC Press, Boca Raton, FL, 1982.
- <sup>19</sup>R.V. McKinney, Jr., and J. Lemons, *The Dental Implant*; pp. 31-50. PSG Publishing, Littleton, MA, 1985.
- <sup>20</sup>E. Dörre and W. Dawihl, "Ceramic Hip Endoprostheses"; pp. 113-27 in *Mechanical Properties of Biomaterials*. Edited by G.W. Hastings and D.F. Williams. Wiley, New York, 1980.
- <sup>21</sup>J.E. Ritter, D.C. Greenspan, R.A. Palmer, and L.L. Hench, "Use of Fracture Mechanics Theory in Lifetime Predictions for Alumina and Bioglass-Coated Alumina," *J. Biomed. Mater. Res.*, **13**, 251-63 (1979).
- <sup>22</sup>R.T. Chiroff, E.W. White, J.N. Webber, and D. Roy, "Tissue Ingrowth of Replamineform Implants," *J. Biomed. Mater. Res. Symp.*, **6**, 29-45 (1975).
- <sup>23</sup>E.W. White, J.N. Webber, D.M. Roy, E.L. Owen, R.T. Chiroff, and R.A. White, "Replamineform Porous Biomaterials for Hard Tissue Implant Applications." *J. Biomed. Mater. Res. Symp.*, **6**, 23-27 (1975).
- <sup>24</sup>R.E. Holmes, R.W. Mooney, R.W. Bucholz, and A.F. Tencer, "A Coralline Hydroxyapatite Bone Graft Substitute," *Clin. Orthop. Relat. Res.*, **188**, 282-92 (1984).
- <sup>25</sup>*Handbook of Bioactive Ceramics*, Vol. II: Calcium Phosphate and Hydroxylapatite Ceramics. Edited by T. Yamamuro, L.L. Hench, and J. Wilson. CRC Press, Boca Raton, FL, 1990.
- <sup>26</sup>S.F. Hulbert and J.J. Klawitter, "Application of Porous Ceramics for the Attachment of Load-Bearing Internal Orthopedic Applications," *Biomed. Mater. Symp.*, **2**, 161-229 (1972).
- <sup>27</sup>S.F. Hulbert, S.J. Morrison, and J.J. Klawitter, "Tissue Reaction to Three Ceramics of Porous and Non-porous Structures," *J. Biomed. Mater. Res.*, **6**, 347-74 (1972).
- <sup>28</sup>S.F. Hulbert, F.W. Cooke, J.J. Klawitter, R.B. Leonard, B.W. Sauer, D.D. Moyle, and H.B. Skinner, "Attachment of Protheses to the Musculo-Skeletal System by Tissue Ingrowth and Mechanical Interlocking," *Biomed. Mater. Symp.*, **4**, 1-23 (1973).
- <sup>29</sup>S.F. Hulbert, J.R. Matthews, J.J. Klawitter, B.W. Sauer, and R.B. Leonard, "Effect of Stress on Tissue Ingrowth into Porous Aluminum Oxide," *Biomed. Mater. Symp.*, **5**, 85-97 (1974).
- <sup>30</sup>L.L. Hench and J.W. Wilson, "Surface-Active Biomaterials." *Science (Washington, D.C.)*, **226**, 630 (1984).
- <sup>31</sup>U. Gross and V. Strunz, "The Interface of Various Glasses and Glass-Ceramics with a Bony Implantation Bed," *J. Biomed. Mater. Res.*, **19**, 251 (1985).
- <sup>32</sup>W. Höhland, W. Vogel, K. Naumann, and J. Gummel, "Interface Reactions Between Machinable Bioactive Glass-Ceramics and Bone," *J. Biomed. Mater. Res.*, **19**, 303 (1985).
- <sup>33</sup>M. Jarcho, "Calcium Phosphate Ceramics as Hard Tissue Prosthetics," *Clin. Orthop. Relat. Res.*, **157**, 259 (1981).
- <sup>34</sup>T. Nakamura, T. Yamamuro, S. Higashi, T. Kokubo, and S. Ito, "A New Glass-Ceramic for Bone Replacement: Evaluation of its Bonding to Bone Tissue," *J. Biomed. Mater. Res.*, **19**, 685 (1985).
- <sup>35</sup>J. Wilson, G.H. Pigott, F.J. Schoen, and L.L. Hench, "Toxicology and Biocompatibility of Bioglass," *J. Biomed. Mater. Res.*, **15**, 805 (1981).
- <sup>36</sup>T. Kokubo, S. Ito, S. Sakka, and T. Yamamuro, "Formation of a High-Strength Bioactive Glass-Ceramic in the System MgO-CaO-SiO<sub>2</sub>-P<sub>2</sub>O<sub>5</sub>," *J. Mater. Sci.*, **21**, 536 (1986).
- <sup>37</sup>T. Kitsugi, T. Yamamuro, and T. Kokubo, "Bonding Behavior of a Glass-Ceramic Containing Apatite and Wollastonite in Segmental Replacement of the Rabbit Tibia Under Load-Bearing Conditions," *J. Bone Jt. Surg., Am. Vol.*, **71A**, 264 (1989).
- <sup>38</sup>S. Yoshii, Y. Kakutani, T. Yamamuro, T. Nakamura, T. Kitsugi, M. Oka, T. Kokubo, and M. Takagi, "Strength of Bonding Between A-W Glass-Ceramic and the Surface of Bone Cortex," *J. Biomed. Mater. Res.*, **22** [A] 327 (1988).
- <sup>39</sup>T. Kokubo, M. Shigematsu, Y. Nagashima, M. Tashiro, T. Nakamura, T. Yamamuro, and S. Higashi, "Apatite- and Wollastonite-Containing Glass-Ceramics for Prosthetic Application," *Bull. Inst. Chem. Res., Kyoto Univ.*, **60**, 260 (1982).
- <sup>40</sup>T. Yamamuro, J. Shikata, Y. Kakutani, S. Yoshii, T. Kitsugi, and K. Ono, "Novel Methods for Clinical Applications of Bioactive Ceramics"; p. 107 in *Bioceramics: Material Characteristics Versus In Vivo Behavior*, Vol. 523. Edited by P. Ducheyne and J.E. Lemons. Annals of New York Academy of Sciences, New York, 1988.
- <sup>41</sup>*Handbook on Bioactive Ceramics*, Vol. I: Bioactive Glasses and Glass-Ceramics. Edited by T. Yamamuro, L.L. Hench, and J. Wilson. CRC Press, Boca Raton, FL, 1990.
- <sup>42</sup>J. Wilson and D. Nolletti, "Bonding of Soft Tissues to Bioglass®"; pp. 283-302 in *Handbook of Bioactive Ceramics*, Vol. I, Bioactive Glasses and Glass-Ceramics. Edited by T. Yamamuro, L.L. Hench, and J. Wilson. CRC Press, Boca Raton, FL, 1990.
- <sup>43</sup>L.L. Hench and H.A. Paschall, "Direct Chemical Bonding Between Bioactive Glass-Ceramic Materials and Bone," *J. Biomed. Mater. Res. Symp.*, **4**, 25-42 (1973).
- <sup>44</sup>L.L. Hench and A.E. Clark, "Adhesion to Bone"; Ch. 6 in *Biocompatibility of Orthopedic Implants*, Vol. 2. Edited by D.F. Williams. CRC Press, Boca Raton, FL, 1982.
- <sup>45</sup>Ö.H. Andersson, G. Liu, K.H. Karlsson, L. Niemi, J. Miettinen, and J. Juhanoja, "In Vivo Behavior of Glasses in the SiO<sub>2</sub>-Na<sub>2</sub>O-CaO-P<sub>2</sub>O<sub>5</sub>-Al<sub>2</sub>O<sub>3</sub>-B<sub>2</sub>O<sub>3</sub> System," *J. Mater. Sci., Mater. Med.*, 219-27 (1990).
- <sup>46</sup>D.C. Greenspan and L.L. Hench, "Chemical and Mechanical Behavior of Bioglass-Coated Alumina," *J. Biomed. Mater. Res.*, **10** [4] 503-509 (1976).
- <sup>47</sup>A.W. Ham, *Histology*, 7th ed; 378-433. Lippincott, Philadelphia, PA, 1969.
- <sup>48</sup>G.W. Hastings and P. Ducheyne, eds., *Natural and Living Biomaterials*; 27-98. CRC Press, Boca Raton, FL, 1984.
- <sup>49</sup>U.M. Gross and V. Strunz, "The Anchoring of Glass Ceramics of Different Solubility in the Femur of the Rat," *J. Biomed. Mater. Res.*, **14**, 607 (1980).
- <sup>50</sup>U. Gross, J. Brandes, V. Strunz, J. Bab, and J. Sela, "The Ultrastructure of the Interface Between a Glass Ceramic and Bone," *J. Biomed. Mater. Res.*, **15**, 291 (1981).
- <sup>51</sup>U. Gross, H.J. Schmitz, V. Strunz, D. Schuppan, and J. Termine, "Proteins at the Interface of Bone-Bonding and Non-Bonding Glass-Ceramics"; p. 98 in Transactions of the Twelfth Annual Meeting of the Society for Biomaterials. Society for Biomaterials, Algonquin, IL, 1986.
- <sup>52</sup>U. Gross, W. Roggendorf, H.J. Schmitz, and V. Strunz, "Testing Procedures for Surface Reactive Biomaterials"; p. 367 in *Biological and Biome-*

- chanical Performance of Biomaterials. Edited by P. Christel, A. Meunier, and A. J. C. Lee. Elsevier, Amsterdam, Netherlands, 1986.
- <sup>53</sup>W. Vogel, W. Hohland, K. Naumann, J. Vogel, G. Carl, W. Gotz, and P. Wange, "Glass-Ceramics for Medicine and Dentistry"; p. 353 in *Handbook of Bioactive Ceramics*, Vol. I, Bioactive Glasses and Glass-Ceramics. Edited by T. Yamamuro, L. L. Hench, and J. Wilson. CRC Press, Boca Raton, FL, 1990.
- <sup>54</sup>Ö. H. Andersson, K. H. Karlsson, K. Kangasniemi, and A. Yti-Urpo, "Models for Physical Properties and Bioactivity of Phosphate Opal Glasses," *Glastech. Ber.*, **61**, 300–305 (1988).
- <sup>55</sup>K. Kangasniemi and A. Yti-Urpo, "Biological Response to Glasses in the  $\text{SiO}_2\text{-Na}_2\text{O-CaO-P}_2\text{O}_5\text{-B}_2\text{O}_3$  System"; pp. 97–108 in *Handbook of Bioactive Ceramics*, Vol. I, Bioactive Glasses and Glass-Ceramics. Edited by T. Yamamuro, L. L. Hench, and J. Wilson. CRC Press, Boca Raton, FL, 1990.
- <sup>56</sup>L. L. Hench, D. B. Spilman, and D. E. Nolletti, "Fluoride Bioglasses®"; pp. 99–104 in *Biological and Biomechanical Performance of Biomaterials*. Edited by P. Christel, A. Meunier, and A. J. C. Lee. Elsevier, Amsterdam, Netherlands, 1986.
- <sup>57</sup>L. L. Hench, H. A. Paschall, W. C. Allen, and G. Piotrowski, "Interfacial Behavior of Ceramic Implants," *Natl. Bur. Stand. Spec. Publ.*, **415**, 19–35 (1975).
- <sup>58</sup>L. L. Hench and H. A. Paschall, "Histological Responses at a Biomaterials Interface," *J. Biomed. Mater. Res.*, **5** [1] 49–64 (1974).
- <sup>59</sup>W. J. McCracken, D. E. Clark, and L. L. Hench, "Aqueous Durability of Lithium Disilicate Glass-Ceramics," *Am. Ceram. Soc. Bull.*, **61** [11] 1218–23 (1982).
- <sup>60</sup>D. E. Clark, C. G. Pantano, and L. L. Hench, *Corrosion of Glass*; pp. 1–7. Books for Industry, Magazines for Industry, Inc., New York, 1979.
- <sup>61</sup>L. L. Hench and D. E. Clark, "Physical Chemistry of Glass Surfaces," *J. Non-Cryst. Solids*, **28**, 83 (1978).
- <sup>62</sup>R. W. Douglas and T. M. El-Shamy, "Reactions of Glasses with Aqueous Solutions," *J. Am. Ceram. Soc.*, **50** [1] 1–8 (1967).
- <sup>63</sup>C. M. Jantzen, "Prediction of Glass Durability as a Function of Environmental Conditions," *Mater. Res. Soc.*, **125**, 143–59 (1988).
- <sup>64</sup>C. M. Jantzen, M. J. Polodinec, and G. G. Wicks, "Thermodynamic Approach to Prediction of the Stability of Proposed Radwaste Glasses"; pp. 491–95 in *Advances in Ceramics*, Vol. 8, *Nuclear Waste Management*. Edited by G. G. Wicks and W. A. Ross. American Ceramic Society, Columbus, OH, 1984.
- <sup>65</sup>B. C. Bunker, D. R. Tallant, T. J. Headley, G. L. Turner, and R. J. Kukpatrick, "The Structure of Leached Sodium Borosilicate Glass," *Phys. Chem. Glasses*, **29** [3] 106–20 (1988).
- <sup>66</sup>A. E. Clark, C. Y. Kim, J. K. West, J. Wilson, and L. L. Hench, "Reactions of Fluoride- and Nonfluoride-Containing Bioactive Glasses"; p. 73 in *Handbook of Bioactive Ceramics*, Vol. I, Bioactive Glasses and Glass-Ceramics. Edited by T. Yamamuro, L. L. Hench, and J. Wilson. CRC Press, Boca Raton, FL, 1990.
- <sup>67</sup>M. Ogino, F. Ohuchi, and L. L. Hench, "Compositional Dependence of the Formation of Calcium Phosphate Films on Bioglass," *J. Biomed. Mater. Res.*, **14**, 55–64 (1980).
- <sup>68</sup>A. E. Clark, C. G. Pantano, and L. L. Hench, "Auger Spectroscopic Analysis of Bioglass Corrosion Films," *J. Am. Ceram. Soc.*, **59** [1–2] 37–39 (1976).
- <sup>69</sup>T. Kokubo, "Surface Chemistry of Bioactive Glass-Ceramics," *J. Non-Cryst. Solids*, **120**, 138–51 (1990).
- <sup>70</sup>Ö. H. Andersson, "The Bioactivity of Silicate Glass"; Ph.D. Dissertation. Department of Chemical Engineering, Åbo Akademi, Finland, 1990.
- <sup>71</sup>C. Y. Kim, A. E. Clark, and L. L. Hench, "Early Stages of Calcium Phosphate Layer Formation in Bioglasses®," *J. Non-Cryst. Solids*, **113**, 195–202 (1989).
- <sup>72</sup>Ö. H. Andersson and K. H. Karlsson, "On the Bioactivity of Silicate Glass," *J. Non-Cryst. Solids*, **129**, 145–51 (1991).
- <sup>73</sup>D. M. Sanders, W. B. Person, and L. L. Hench, "Quantitative Analysis of Glass Structure Using Infrared Reflection Spectra," *Appl. Spectrosc.*, **28** [3] 247–55 (1974).
- <sup>74</sup>B. O. Fowler, "Infrared Studies of Apatites. I. Vibrational Assignments for Calcium, Strontium, and Barium Hydroxyapatite Utilizing Isotopic Substitution," *Inorg. Chem.*, **13** [1] 194 (1974).
- <sup>75</sup>R. F. Le Geros, G. Bone, and R. Le Geros, "Type of H<sub>2</sub>O in Human Enamel and in Precipitated Apatites," *Calcif. Tissue Res.*, **26**, 111 (1978).
- <sup>76</sup>L. L. Hench, "Stability of Ceramics in the Physiological Environment"; pp. 67–85 in *Fundamental Aspects of Biocompatibility*, Vol. 1. Edited by D. F. Williams. CRC Press, Boca Raton, FL, 1981.
- <sup>77</sup>T. Kokubo, "Bonding Mechanism of Bioactive Glass-Ceramic A-W to Living Bone"; pp. 41–50 in *Handbook of Bioactive Ceramics*, Vol. I, Bioactive Glasses and Glass-Ceramics. Edited by T. Yamamuro, L. L. Hench, and J. Wilson. CRC Press, Boca Raton, FL, 1990.
- <sup>78</sup>C. Oktsuki, T. Kokubo, K. Takatsuka, and T. Yamamuro, "Compositional Dependence of Bioactivity of Glasses in the System  $\text{CaO-SiO}_2\text{-P}_2\text{O}_5$  and its In Vitro Evaluation," *Nippon Seramikkusu Kyokai Gakujutsu Ronbunshi*, **99** [1] 1–6 (1991).
- <sup>79</sup>R. Li, A. E. Clark, and L. L. Hench, "An Investigation of Bioactive Glass Powders by the Sol-Gel Process"; p. 40 in *Transactions of 16th Annual Meeting of the Society for Biomaterials* (Charleston, SC, May 20–23, 1990), Vol. XIII. Society for Biomaterials, Algonquin, IL, 1990.
- <sup>80</sup>M. M. Walker, "An Investigation into the Bonding Mechanisms of Bioglass"; M.S. Thesis. University of Florida, Gainesville, FL, 1977.
- <sup>81</sup>M. Jarcho, "Calcium Phosphate Ceramics as Hard Tissue Prosthetics," *Clin. Orthop. Relat. Res.*, **157**, 259 (1981).
- <sup>82</sup>D. F. Williams, "The Biocompatibility and Clinical Uses of Calcium Phosphate Ceramics"; pp. 43–66 in *Biocompatibility of Tissue Analogs*, Vol. II. Edited by D. F. Williams. CRC Press, Boca Raton, FL, 1985.
- <sup>83</sup>J. E. Davies, "The Use of Cell and Tissue Culture to Investigate Bone Cell Reactions to Bioactive Materials"; p. 195 in *Handbook of Bioactive Ceramics*, Vol. I, Bioactive Glasses and Glass-Ceramics. Edited by T. Yamamuro, L. L. Hench, and J. Wilson. CRC Press, Boca Raton, FL, 1990.
- <sup>84</sup>J. E. Davies, ed., *Proceedings of the Bone-Biomaterials Interface Workshop* (Toronto, Ontario, Canada, December 3–4, 1990). University of Toronto Press, Toronto, Ontario, Canada, in press.
- <sup>85</sup>R. Reck, S. Storckel, and A. Meyer, "Bioactive Glass-Ceramics in Middle Ear Surgery: An 8-Year Review"; p. 100 in *Bioceramics: Materials Characteristics Versus In Vivo Behavior*, Vol. 523. Edited by P. Ducheyne and J. Lemons. Annals of New York Academy of Sciences, New York, 1988.
- <sup>86</sup>G. E. Merwin, "Review of Bioactive Materials for Otolgic and Maxillofacial Applications"; pp. 323–28 in *Handbook of Bioactive Ceramics*, Vol. I, Bioceramic Glasses and Glass Ceramics. Edited by T. Yamamuro, L. L. Hench, and J. Wilson. CRC Press, Boca Raton, FL, 1990.
- <sup>87</sup>E. Douek, "Otolgic Applications of Bioglass® Implants"; in *Proceedings of IVth International Symposium on Bioceramics in Medicine* (London, U.K., Sept. 10–11, 1991) Edited by W. Bonfield. Butterworth-Heinemann, Ltd., London, U.K., 1991, in press.

<sup>88</sup>T. Yamamuro, "Reconstruction of the Iliac Crest with Bioactive Glass-Ceramic Prostheses"; pp. 335-42 in *Handbook of Bioactive Ceramics*, Vol. I, Bioactive Glasses and Glass Ceramics. Edited by T. Yamamuro, L.L. Hench, and J. Wilson. CRC Press, Boca Raton, FL, 1990.

<sup>89</sup>T. Yamamuro, "Replacement of the Spine with Bioactive Glass-Ceramic Prosthesis"; pp. 343-52 in *Handbook of Bioactive Ceramics*, Vol. I, Bioactive Glasses and Glass-Ceramics. Edited by T. Yamamuro, L.L. Hench, and J. Wilson. CRC Press, Boca Raton, FL, 1990.

<sup>90</sup>H.R. Stanley, M.B. Hall, A.E. Clark, G.E. Turner, F. Colaizzi, L.L. Hench, and C. King, "Alveolar Ridge Maintenance Using Endosseously Placed Bioglass® (45S5 Cones)"; to be published in 1992.

<sup>91</sup>J. Walliker, H. Carson, E.E. Douek, A. Fourcin, and S. Rosen; p. 265 in *Proceedings of Cochlear Implant Symposium*. Edited by P. Banfai. Dürer, FRG, Sept. 7-12, 1987.

<sup>92</sup>M. Jarcho, J.I. Kay, R.H. Gummaer, and H.P. Drobeck, "Tissue, Cellular, and Subcellular Events at a Bone-Ceramic Hydroxylapatite Interface," *J. Biomat.*, **1**, 79 (1977).

<sup>93</sup>M. Ogiso, H. Kaneda, J. Arasaki, I. Tabata, and T. Hidaka, "Epithelial Attachment and Bone Tissue Formation on the Surface of Hydroxylapatite Ceramics"; p. 4.1.5 in *Proceeding of 1st World Biomaterials Congress* (Baden, Austria, 1980). European Society for Biomaterials, 1980.

<sup>94</sup>M. Ogiso, H. Kaneda, J. Arasaki, K. Ishida, M. Shiota, T. Mitsuwa, T. Tabata, Y. Yamazaki, and T. Hidaka, "Hydroxyapatite Ceramic Implants under Occlusal Function"; p. 54 in *Transactions of the 4th Annual Meeting of the Society for Biomaterials* (Rensselaer, NY, May 28-31, 1981). Society for Biomaterials, Algonquin, IL, 1981.

<sup>95</sup>H. Aoki, Y. Shin, and M. Akao, "Sintered Hydroxyapatite for a Percutaneous Device"; p. 1 in *Advances in Biomaterials*, Vol. 6. Edited by P. Ducheyne, P. Christel, A. Meunier, and A.T.C. Lee. Elsevier, New York, 1986.

<sup>96</sup>N. Yoshiyama, Y. Shin, and H. Aoki, "Hydroxylapatite Percutaneous Access Device in Peritoneal Dialysis"; p. 377 in *Handbook of Bioactive Ceramics*, Vol. II, Calcium Phosphate and Hydroxylapatite Ceramics. Edited by T. Yamamuro, L.L. Hench, and J. Wilson. CRC Press, Boca Raton, FL, 1990.

<sup>97</sup>T. Tsuji, H. Aoki, Y. Shin, and T. Togawa, "Implantation in the Human Forearm of a Percutaneous Device Made of Sintered Hydroxylapatite"; pp. 383-76 in *Handbook of Bioactive Ceramics*, Vol. II, Calcium Phosphate and Hydroxylapatite Ceramics. Edited by T. Yamamuro, L.L. Hench, and J. Wilson. CRC Press, Boca Raton, FL, 1990.

<sup>98</sup>J. Wilson, "Preface"; in *Handbook of Bioactive Ceramics*, Vols. I and II. Edited by T. Yamamuro, L.L. Hench, and J. Wilson. CRC Press, Boca Raton, FL, 1990.

<sup>99</sup>C. Doyle, "Bioactive Composites in Orthopedics"; pp. 195-208 in *Handbook of Bioactive Ceramics*, Vol. II, Calcium Phosphate and Hydroxylapatite Ceramics. Edited by T. Yamamuro, L.L. Hench, and J. Wilson. CRC Press, Boca Raton, FL, 1990.

<sup>100</sup>P. Ducheyne and J.F. McGucken, Jr., "Composite Bioactive Ceramic-Metal Materials"; pp. 185-86 in *Handbook of Bioactive Ceramics*, Vol. II, Calcium Phosphate and Hydroxylapatite Ceramics. Edited by T. Yamamuro, L.L. Hench, and J. Wilson. CRC Press, Boca Raton, FL, 1990.

<sup>101</sup>U. Solte, "Ceramics in Composites: Review and Current Status"; pp. 137-56 in *Bioceramics: Materials Characteristics vs In Vivo Behavior*, Vol. 523. Edited by P. Ducheyne and J.E. Lemons. Annals of New York Academy of Sciences, New York, 1988.

<sup>102</sup>W. Bonfield, "Hydroxyapatite-Reinforced

Polyethylene as an Analogous Materials for Bone Replacement"; pp. 173-77 in *Bioceramics: Materials Characteristics vs In Vivo Behavior*, Vol. 523. Edited by P. Ducheyne and J.E. Lemons. Annals of New York Academy of Sciences, New York, 1988.

<sup>103</sup>J.C. Behiri and W. Bonfield, "Fracture Mechanics of Bone: The Effects of Density, Specimen Thickness, and Crack Velocity on Longitudinal Fracture," *J. Biomech.*, **17**, 25 (1984).

<sup>104</sup>W. Bonfield, C. Doyle, and K.E. Tanner, "In Vivo Evaluation of Hydroxyapatite-Reinforced Polyethylene Composites"; p. 153 in *Biological and Biomechanical Performance of Materials*. Edited by P. Christel, A. Meunier, and A.J.C. Lee. Elsevier, New York, 1986.

<sup>105</sup>A.F. Tencer, R.L. Woodard, J. Swenson, and K.L. Brown, "Mechanical and Bone Ingrowth Properties of a Polymer-Coated, Porous, Synthetic, Coralline Hydroxyapatite Bone-Graft Materials"; p. 153 in *Bioceramics: Materials Characteristics vs In Vivo Behavior*, Vol. 523. Edited by P. Ducheyne and J.E. Lemons. Annals of New York Academy of Sciences, New York, 1988.

<sup>106</sup>T. Kasuga, K. Nakajima, T. Uno, and M. Yoshida, "Bioactive Glass-Ceramic Composite Toughened by Tetragonal Zirconia"; pp. 137-42 in *Handbook of Bioactive Ceramics*, Vol. I, Bioceramic Glasses and Glass Composites. Edited by T. Yamamuro, L.L. Hench, and J. Wilson. CRC Press, Boca Raton, FL, 1990.

<sup>107</sup>P. Ducheyne and L.L. Hench, "The Processing of Static Mechanical Properties and Metal Fibre-Reinforced Bioglass," *J. Mater. Sci.*, **17**, 595-606 (1982).

<sup>108</sup>E. Schepers, P. Ducheyne, and M. DeClerk, "Interfacial Analysis of Fiber-Reinforced Glass Dental Root Implants." *J. Biomed. Mater. Res.*, **23**, 735-52 (1989).

<sup>109</sup>J.C. Bokros, U.S. Pat. No. 3526005, 1971.

<sup>110</sup>J.C. Bokros, "Carbon Biomedical Devices," *Carbon*, **15**, 355-71 (1977).

<sup>111</sup>A. Haubold, H.S. Shim, and J.C. Bokros, "Carbon in Medical Devices"; pp. 3-42 in *Biocompatibility of Clinical Implant Materials*, Vol. II. CRC Press, Boca Raton, FL, 1981.

<sup>112</sup>J.D. Bokros, "Carbon Biomedical Devices," *Carbon*, **18**, 355-71 (1977).

<sup>113</sup>A.D. Haubold, R.A. Yapp, and J.D. Bokros, "Carbons"; pp. 95-101 in *Concise Encyclopedia of Medical and Dental Materials*. Edited by D. Williams. Pergamon Press, New York, 1990.

<sup>114</sup>S.D. Cook, "In Vivo Evaluation of Hydroxylapatite Coatings for Orthopedic and Dental Applications"; in *Proceedings of 3rd International Symposium on Bioceramics in Medicine* (Rose Hulman Institute of Technology, Terre Haute, IN, Nov. 18-20, 1990). Edited by S.F. Hulbert. Moore-Langen, Terre Haute, IN, 1991, in press.

<sup>115</sup>G. Boos, M. Thirwell, R. Blanchard, C. Cryps, M. Herba, L. Gonzales, L. Rosenthal, J. Skelton, and G. Borleau; presented at 25th Annual Meeting of the American Society Clinical Oncology, San Francisco, CA, May 21-23, 1989.

<sup>116</sup>D. Day; personal communication, 1991.

<sup>117</sup>K. Ohara, M. Ikenaga, T. Nakamura, and T. Yamamuro, "Heat-Generating Bioactive Ceramics," *J. Biomed. Mater.*, **25**, 357-65 (1991).

<sup>118</sup>H.A. Benghuzzi and P.K. Bajpai, "Sustained Release of Steroid Hormones from Polylactic Acid or Polycaprolactone-Impregnated Ceramics"; pp. 93-110 in *Handbook of Bioactive Ceramics*, Vol. II, Calcium Phosphate and Hydroxylapatite Ceramics. Edited by T. Yamamuro, L.L. Hench, and J. Wilson. CRC Press, Boca Raton, FL, 1990.

<sup>119</sup>W.R. Lacefield and L.L. Hench, "The Bonding of Bioglass® to a Cobalt-Chromium Surgical Implant Alloy," *Biomaterials*, **7** [2] 104-108 1986.

<sup>120</sup>F.G. Evans and A. King, *Biomechanical Studies of the Musculoskeletal System*; pp. 49-53

Charles C. Thomas, Springfield, IL, 1961.

<sup>121</sup>W. Bonfield, "Elasticity and Viscoelasticity of Cortical Bone"; pp. 43–60 in *Natural and Living Biomaterials*. Edited by G.W. Hastings and P. Ducheyne. CRC Press, Boca Raton, FL, 1984.

<sup>122</sup>R. Van Audekercke and M. Martens, "Mechanical Properties of Cancellous Bone"; pp. 89–98 in *Natural and Living Biomaterials*. Edited by G.W. Hastings and P. Ducheyne. CRC Press, Boca Raton, FL, 1984. □



Larry L. Hench graduated from The Ohio State University in 1961 and 1964 with B.S. and Ph.D. degrees in ceramic engineering. He joined the faculty of the University of Florida in 1964 where

he now serves as Graduate Research Professor of Materials Science and Engineering, Director of the Bioglass® Research Center, and Co-Director of the Advanced Materials Research Center. Professor Hench discovered Bioglass®, the first synthetic material to bond with living tissues, in 1969. During 1978 to 1985, he and his students conducted a series of basic science studies on glasses to immobilize high-level radioactive wastes, including the first deep geological burial in Sweden. In 1980, Professor Hench initiated study of low-temperature sol-gel processing of glasses, ceramics, and composites, which led to new classes of silica materials for optics termed Gelsil®. Professor Hench's studies have resulted in more than 300 scientific publications, 19 books, 20 U.S. patents, and 20 foreign patents. He is a member of the American Ceramic Society, Academy of Ceramics, and Society of Biomaterials; he has served in a variety of offices and has received awards from these and other academic and scientific institutions.